# Divergent Fe-Mediated C–H Activation Paths Driven by Alkali Cations

Vincent Wowk, Alexis K Bauer, Aleksa Radovic, Lise-Marie Chamoreau, Michael L Neidig, Guillaume Lefèvre

JACS Au
AN OPEN ACCESS JOURNAL OF THE AMERICAN CHEMICAL SOCIETY



pubs.acs.org/jacsau
Article

# Divergent Fe-Mediated C−H Activation Paths Driven by Alkali Cations

Vincent Wowk, Alexis K. Bauer, Aleksa Radovic, Lise-Marie Chamoreau, Michael L. Neidig,* and Guillaume Lefèvre*

Cite This: *JACS Au* 2024, 4, 512−524

Read Online

ACCESS | Metrics & More | Article Recommendations | Supporting Information

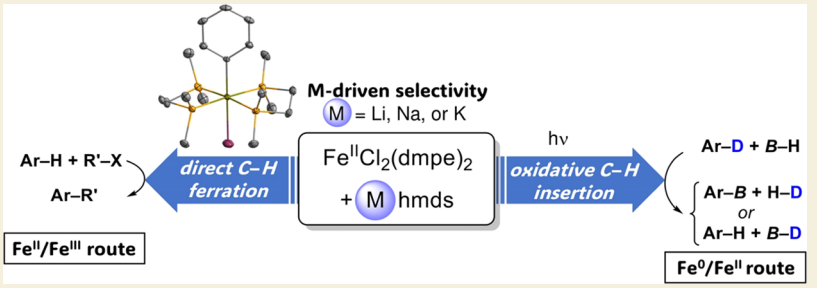


**ABSTRACT:** The association of the ferrous complex $Fe^{II}Cl_2(dmpe)_2$ (**1**) with alkali bases M(hmds) (M = Li, Na, K) proves to be an efficient platform for the activation of Ar−H bonds. Two mechanisms can be observed, leading to either Ar−$Fe^{II}$ species by deprotonative ferration or hydrido species Ar−$Fe^{II}$−H by oxidative addition of transient $Fe^0(dmpe)_2$ generated by reduction of **1**. Importantly, the nature of the alkali cation in M(hmds) has a strong influence on the preferred path. Starting from the same iron precursor, diverse catalytic applications can be explored by a simple modulation of the $M^I$ cation. Possible strategies enabling cross-coupling using arenes as pro-nucleophiles, reductive dehydrocoupling, or deuteration of B−H bonds are discussed.

**KEYWORDS:** *iron, C−H activation, cross-coupling, dehydrocoupling, boranes, mechanisms*

## INTRODUCTION

Metalation of C−H bonds by transition metals (TMs) is a pivotal transformation in organometallic catalysis, leading to reactive organotransition species. Such compounds are key intermediates in numerous classic transformations such as cross-couplings, carbometalations, electrophilic additions, etc. Moreover, use of hydrocarbons as pro-nucleophiles in metalation processes is a more atom-economic alternative to main-group nucleophiles (e.g., RMgX, RZnX, RLi, etc.) used as transmetalation reagents.[1]

Catalytic processes relying on a C−H metalation step with a TM source usually require the C−H bond target to be turned as a metalated intermediate at each catalytic cycle. Among this variety of organometallic species, organoiron compounds featuring well-defined C−Fe bonds have kept drawing particular attention during the last few decades.[2] Indeed, iron catalysts are appealing candidates for synthetic applications, since they are a sustainable and cheap alternative to noble metals.[3] Formation of well-defined organoiron compounds is still particularly challenging due to the intrinsic instability of the C−Fe bond. For the same reason, a fine mechanistic analysis of the reactivity patterns followed by such species is also a delicate question.[4] Indeed, depending on the iron oxidation state, C−Fe bonds can undergo fast homolytic cleavage,[5] and two-electron reductive eliminations also easily occur from multiple coordinated $R_n[Fe^{II}]$ complexes.[6]

Two very distinct strategies can be adopted for the generation of C−Fe bonds from C−H substrates and are particularly applied to the activation of Ar−H bonds. The first one relies on a direct ferration of the C−H bond, which is deprotonated by a suitable base at a Lewis-acidic iron center (Scheme 1a). Classic directed deprotonative ferrations were for example reported by Knochel, using $Fe^{II}(TMP)_2{\cdot}2MgCl_2{\cdot}4LiCl$ (TMP = 2,2,6,6-tetramethylpiperidine).[7] Nakamura also reported an efficient aryl−aryl cross-coupling involving a directed $C_{Ar}$−H deprotonation mediated by PhMgBr in the presence of a $Zn^{II}$ source, the iron catalyst being associated with 1,10-phenanthroline;[8a] the same group also recently reported improved methods of C−H functionalizations relying on a key deprotonative ferration.[8b−d] Similarly, Neidig and Ackermann demonstrated that directed $C_{Ar}$−H activation of triazole derivatives at an $Fe^{II}$ intermediate followed by cross-

Received: October 24, 2023
Revised: December 20, 2023
Accepted: December 20, 2023
Published: January 19, 2024

**Scheme 1. Classic Strategies for the Generation of C−Fe Bonds**[a]

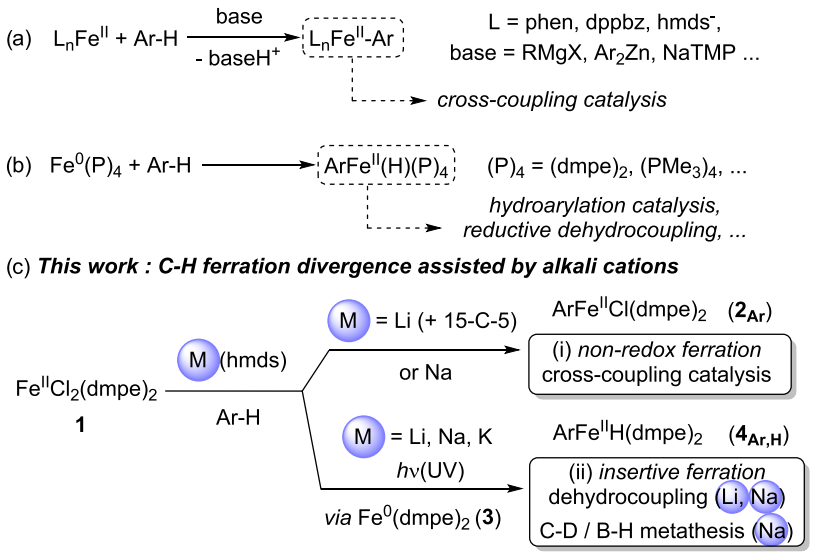


[a](a) Deprotonative ferration; (b) oxidative insertion; (c) this work: non-redox and oxidative ferrations unlocked by alkali additives.

coupling can be mediated by the $Ar_2Zn$/dppbz combination (dppbz = 1,2-bis(diphenylphosphino)benzene).[9] Hevia recently reported an example of nondirected ferration of unactivated arenes (including $C_6H_6$) using $Fe^{II}(hmds)_2$ ($hmds^- = N(SiMe_3)_2^-$) and NaTMP relying on a cooperative effect between the $Fe^{II}$ and $Na^I$ cations.[10]

A second strategy consists in the ferration of C−H bonds by oxidative insertion of a $Fe^0$ complex, leading to the formation of heteroleptic hydrido-organoiron(II) species (Scheme 1b). Early reports by Field and Tolman showed that transient $Fe^0(dmpe)_2$ (dmpe = 1,2-bis(dimethylphosphino)ethane) generated by photolysis of the ferrous precursor $Fe^{II}(R)(R')(dmpe)_2$ (R,R′ = H, Me or 2-Np, H) easily underwent insertion into a variety of $C_{sp^2}$−H and $C_{sp^3}$−H bonds.[11] Similar $Fe^0(P)_4$ systems have been reported ever since. It was also recently demonstrated that in situ generated $Fe^0(dmpe)_2$ was an efficient catalyst for the reductive dehydrocoupling of $C_{Ar}$−H and B−H bonds in order to access arylpinacolboranes Ar−B(pin),[12a] or for hydrogen isotopic exchange (HIE) between alkenes or arenes and $CD_3OD$.[12b] In the latter case, $Fe^0(dmpe)_2$ is generated from **1** in the presence of pinacolborane (pinBH) and $CD_3OD$ under blue light irradiation. $Fe^0(PMe_3)_4$ also proved to efficiently promote *ortho*-directed insertion into $C_{Ar}$−H bonds[13] and was successfully used by several groups such as Kakiuchi's and Ackermann's as a catalyst for the addition of Ar−H bonds onto alkenes[14] and allenes,[15] or for the homoallylation of aryl ketones using methylenecyclopropanes.[16]

The two activation pathways of a $C_{Ar}$−H bond depicted in Scheme 1a,b lead to strongly different aryliron(II) intermediates. In the first case, the H atom coming from the activated $C_{Ar}$−H bond acts as a proton $H^+$ trapped by a basic partner and is not transferred onto the final product (Scheme 1a). Conversely, in the second case, this H atom affords a Fe-bound hydride $H^-$, the formal two-electron reduction of the $C_{Ar}$−H bond being ensured by the $Fe^0/Fe^{II}$ couple. This leads to possible catalytic transformations in which both the Ar group and the H atom are transferred onto a suitable target (Scheme 1b). The two aforementioned strategies (that is nonredox deprotonation, Scheme 1a, or two-electron oxidative insertion, Scheme 1b) usually require drastically different iron precursors and are extremely sensitive to ligand effects. Moreover, generation of efficient precursors of $Fe^0(dmpe)_2$ demands the prior multistep synthesis and purification of extremely air-sensitive complexes such as $Fe^{II}(R)_2(dmpe)_2$ (R = H, Me) or $Fe^{II}(2\text{-Np})(H)(dmpe)_2$, the latter being formed by reduction of $FeCl_2(dmpe)_2$ (**1**) by sodium naphthalenide (NaNp).[11a]

In this report, we demonstrate that the well-known, easily accessible complex $FeCl_2(dmpe)_2$ (**1**) can be associated with alkali amides M(hmds) (M = Li, Na, K) to perform nondirected $C_{Ar}$−H activations by either deprotonative or oxidative addition paths (Scheme 1c, paths i−ii). Ar−[$Fe^{II}$] compounds formed by deprotonation can be active in cross-coupling with organic iodides, a key demetalation of a dmpe ligand being ensured by Lewis-acidic cations such as $Li^I$ (as well as $Mg^{II}$) in the catalytic process. When Ar−[$Fe^{II}$]−H compounds are obtained, use of $Li^I$ salts can selectively promote the borylation of Ar−H into Ar−B(pin) by a Ar−H/(pin)B−H dehydrocoupling. On the other hand, use of $Na^I$ salts affords a near equimolar mixture of $Ar_D$−B(pin) borylation product along with hydrogen isotopic exchange (HIE) between $C_6D_6$ and (pin)B−H (formation of (pin)B−D).

This finding opens the door to particularly appealing synthetic strategies, since a simple ferrous precursor **1**, readily synthesized from commercially available $FeCl_2$ and dmpe, combined with the suitable alkali salt M(hmds), can be used as a single precursor for generating organoiron species active in either cross-coupling or in dehydrocoupling/HIE catalysis. The role of the alkali cation in the speciation of the iron-containing species formed by action of M(hmds) on the precursor **1** is discussed. Characterization of key $C_{Ar}$−H activated products featuring Ar−$Fe^{II}$ bonds was probed by $^{31}P$ and $^1H$ NMR spectroscopies, X-ray diffraction, and Mössbauer spectroscopy.

## Speciation of the Iron-Containing Species upon Treatment of 1 by M(hmds) (M = Li, Na, K)

We began by investigating the distribution of species, which can be formed under treatment of **1** by M(hmds) (M = Li, Na,


https://doi.org/10.1021/jacsau.3c00649
JACS Au 2024, 4, 512−524

**Table 1. Speciation of Complexes 1−5 Obtained by Treatment of 1 by *n* equiv of M(hmds) (M = Li, Na, K) under Various Conditions**

| $(C_6D_5)Fe^{II}Cl(dmpe)_2$ | $Fe^0{}_2(dmpe)_5$ | $Fe^0(dmpe)_3$ | $(C_6D_5)Fe^{II}D(dmpe)_2$ | $Fe^{II}(hmds)_3^{\ominus}$ |
|---|---|---|---|---|
| $\mathbf{2_{C6D5}}$ | **3'** | **3''** | $\mathbf{4_{C6D5,D}}$ | $\mathbf{5^{\ominus}}$ |

| entry | M (*n*) | *t* (h) | *T* (°C) | solvent[a] | light | **1** | $\mathbf{2_{C6D5}}$ | **3′** | **3″** | $\mathbf{4_{C6D5,D}}$ | $\mathbf{5^-}$ |
|---|---|---|---|---|---|---|---|---|---|---|---|
| 1 | Li (2) | 72 | 20 | $C_6D_6$ | no | 97 | 0 | 0 | 0 | 0 | 2 |
| 2 | Na (2) | 72 | 20 | $C_6D_6$ | no | 0 | 0 | 40 | 7 | 5 | 4 |
| 3 | K (2) | 72 | 20 | $C_6D_6$ | no | 5 | 0 | 10 | 20 | 4 | 7 |
| 4 | Li (2) | 72 | 20 | $C_6D_6$ | yes | 5 | 0 | 0 | 0 | 40[b] | 0 |
| 5 | Na (2) | 72 | 20 | $C_6D_6$ | yes | 0 | 0 | 0 | 0 | 48[b] | 2 |
| 6 | K (2) | 72 | 20 | $C_6D_6$ | yes | 5 | 0 | 0 | 0 | 45[b] | 5 |
| 7 | Li (10) | 22 | 20 | $C_6D_6$/THF | no | 97 | 0 | 0 | 0 | 0 | 2 |
| 8 | Na (10) | 22 | 20 | $C_6D_6$/THF | no | 0 | 7 | 16 | 8 | 5 | 3 |
| 9 | K (10) | 22 | 20 | $C_6D_6$/THF | no | 0 | 0 | 8 | 4 | 3 | 10 |
| 10 | Li (10) | 22 | 80 | $C_6D_6$/THF | no | 0[c] | 0[c] | 0[c] | 0[c] | 0[c] | 18[c] |
| | | | | | | 0[d] | 0[d] | 0[d] | 0[d] | 38[b,d] | 15[b,d] |
| 11 | Na (10) | 22 | 80 | $C_6D_6$/THF | no | 0 | 0 | 12 | 13 | 0 | 0 |
| 12 | K (10) | 22 | 80 | $C_6D_6$/THF | no | 0 | 0 | 7 | 5 | 0 | 2 |

[a]Neat $C_6D_6$ or a 9:1 mixture of $C_6D_6$/THF were used. [b]Mixture of *cis*:*trans*-$\mathbf{4_{C6D5,D}}$ in a ca. 4:3 ratio. [c]Spectra recorded after cooling down the samples at room temperature during 1 h. [d]Spectra recorded after 10 additional hours at room temperature.

K) in $C_6D_6$ at room temperature, under thermal activation (80 °C) or under UV irradiation (365 nm). Our main objective was to evidence the different C−D activation compounds that can be formed under those conditions. Treatment of **1** by M(hmds) in $C_6D_6$ can afford a distribution of species, which for some of them have been previously described in the literature (complexes **2**−**5**, Table 1).[17]

In neat $C_6D_6$, **1** remained mostly unreacted upon action of 2 equiv of Li(hmds) after 72 h at room temperature (97%, Table 1, entry 1), and less than 5% of $\mathbf{5^-}$ were formed. On the other hand, action of 2 equiv of Na(hmds) under the same conditions led to an almost total conversion of **1**. Reduced $Fe^0$ complexes **3′** and **3″** were obtained (respectively 40 and 7%, entry 2), as well as the C−D activated complex $\mathbf{4_{C6D5,D}}$ (5%). Formation of traces of the latter suggests that transient $Fe^0(dmpe)_2$ (**3**) was obtained under those conditions, followed by oxidative insertion in the C−D bond of $C_6D_6$ (Scheme 1c, path (ii)). Use of K(hmds) (entry 3) afforded a similar distribution of **3′**, **3″**, and $\mathbf{4_{C6D5,D}}$ (respectively, 10, 20, and 4%). It is of note that the possibility to use K(hmds) as a reductant of ferrous complexes stabilized by noninnocent coordinating platforms has already been reported in the past.[18a] Similarly, Lei demonstrated that Na(hmds) was able to perform one-electron reduction of $Cu^{II}$ salts into dicoordinated $Cu^{I}(hmds)_2^-$.[18b] Moreover, the sole detection of $NH(SiMe_3)_2$ as an organic byproduct by GC-MS also suggests that the alkali amides used in the reduction course of **1** described herein promote formation of the $Fe^0$ stage by successive one-electron transfers. The lack of reactivity of Li(hmds), compared to that of Na(hmds) and K(hmds), can be explained by the kinetic inertia of **1** (low-spin $d^6$ octahedral complex[19]) and the strong electrostatic lithium/amide interaction existing in Li(hmds), which will slow down any reaction of Li(hmds) with the ferrous ion. Given that alkali cations can lead to the formation of $\pi$-arene adducts in the presence of an aromatic solvent ($C_6D_6$ herein),[20] the same experiments were carried out in the presence of a more donating solvent ($C_6D_6$/THF 9:1 mixture). No significant variations were obtained, meaning that reducing properties of Na(hmds) and K(hmds) remained unchanged under those conditions (Figures S15−S17). Treatment of **1** by 2 equiv of M(hmds) was then performed under UV irradiation ($\lambda$ = 365 nm) during 72 h at room temperature. In all cases (respectively M = Li, Na, or K, entries 4−6), complex $\mathbf{4_{C6D5,D}}$ was detected in significant quantities (respectively, 40, 48, and 45%) and was the major species detected by NMR along with traces of $\mathbf{5^-}$ and unreacted **1**. In other words, this means that a clean reduction of **1** by 2 equiv of M(hmds) into transient **3** can be triggered by UV irradiation, affording $\mathbf{4_{C6D5,D}}$ by oxidative insertion. Formation of **3** by photolytic evolution of reactive sensitive precursors such as $Fe^{II}(R)(R')(dmpe)_2$ (R,R′ = H, Me or 2-Np, H) has already been used and described in the past.[11,12a] However, accessing **3** by reduction of a stable, easily handled precursor such as **1** in the presence of reductants classically used in synthetic chemistry such as M(hmds) is an appealing alternative to the use of the aforementioned sensitive precursors. A previous example of in situ activation of $FeCl_2(dmpe)_2$ in **3** by *t*BuOK had been reported by the group of Thomas in 2022.[12b]

The action of an excess of M(hmds) on **1** at room temperature (10 equiv during 22 h) was then investigated (entries 7−9). In that case, a $C_6D_6$/THF 9:1 mixture was used, in order to circumvent solubility issues, which precluded the obtention of interpretable NMR spectra. Almost no conversion was observed with Li(hmds) (entry 7). Reduction by Na(hmds) (respectively K(hmds)) afforded ca. 25% of **3′** and **3″** (respectively 12%, entries 8−9) and 3% of complex $\mathbf{5^-}$ (respectively 10%). Traces of $\mathbf{4_{C6D5,D}}$ were observed for both Na(hmds) and K(hmds). Overall, the amount of NMR-detected species is smaller with 10 equiv of M(hmds) than with 2 equiv of the latter (M = Na, K; compare entries 8−9 and 2−3).[21] However, in the case of Na(hmds) (entry 8), ca. 7% of complex $(C_6D_5)Fe^{II}(Cl)(dmpe)_2$ ($\mathbf{2_{C6D5}}$) was also observed, with its diagnostic signal at $\delta$ = 67 ppm in $^{31}P$ NMR.[11b] Detection of small amounts of $\mathbf{2_{C6D5}}$ thus shows that Na(hmds) also enables C−D activation of $C_6D_6$ by nonredox deprotonation path i (Scheme 1c).

At a higher temperature (80 °C), reduction of **1** by 10 equiv of Na(hmds) (respectively K(hmds)) afforded a mostly NMR-silent distribution (entries 11−12), with reduced **3′**, **3″** quantities roughly similar to what was obtained at room


https://doi.org/10.1021/jacsau.3c00649
JACS Au 2024, 4, 512−524

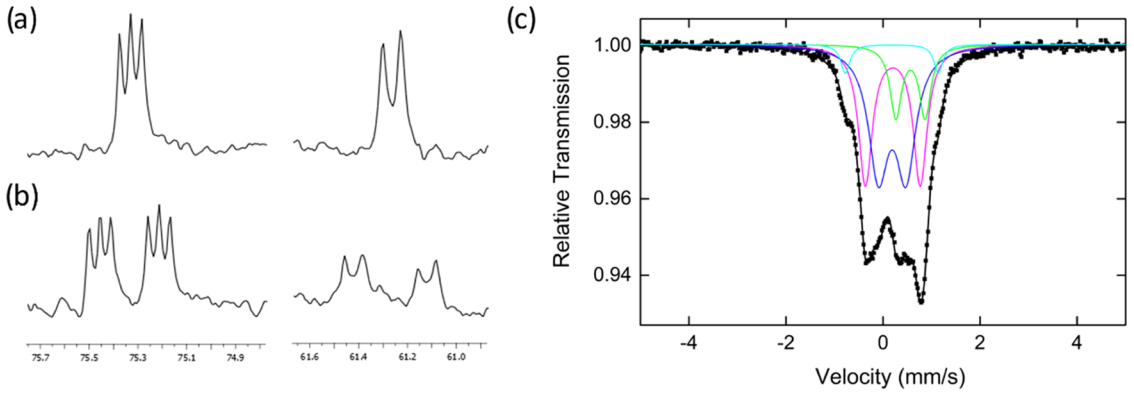


**Figure 1.** $^{31}$P NMR patterns of (a) $\mathbf{4}_{C6D5,D}$; **3*** and (b) $^{57}$**Fe-4**$_{C6D5,D}$; $^{57}$**Fe-3*** obtained after thermolysis of respectively **1** and $^{57}$**Fe-1** in $C_6D_6$ in the presence of 10 equiv of Li(hmds) during 22 h at 80 °C; spectra recorded after 10 additional hours at 20 °C, see Figure S33 for the full spectra; (c) 80 K $^{57}$Fe Mössbauer spectrum of a frozen solution corresponding to spectrum (b).

temperature. This distribution did not evolve after 10 h at room temperature. This means that the NMR-silent ill-defined reduced iron species obtained in that case are not able to promote the formation of $\mathbf{4}_{C6D5,D}$. The situation was strongly different when Li(hmds) was used (10 equiv per mole of **1**, at 80 °C during 22 h, entry 10). $\mathbf{5}^-$ (18%) is the sole species detected under these conditions and is almost undetected with Na(hmds) or K(hmds). This highlights the enhanced stability of $\mathbf{5}^-$ in the presence of $Li^I$ countercations, likely by the formation of a tight {$\mathbf{5}^-$;$\mathbf{Li}^+$} ion pair. However, the speciation progressively evolves at room temperature (Figure S33), and $\mathbf{4}_{C6D5,D}$ is detected after 10 additional hours at 20 °C (ca. 38%, *cis*:*trans* = 4:3, Figure 1a, and Table 1, entry 10, note d) additionally to $\mathbf{5}^-$, which remains almost unreacted (15%). New species **3*** (ca. 10%), which displays $^{31}$P resonances similar to that of $Fe_2^0(dmpe)_5$ (**3′**), is also detected (Figure 1a,b; a classic splitting of those signals upon use of $^{57}$Fe-labeled material is observed, confirming the presence of one Fe atom in **3***).[22] Additionally, broad resonances in the 50−60 ppm range are also observed and do not display any particular additional splitting upon $^{57}$Fe-labeling experiments (Figure S33). Given that this area can correspond to diamagnetic $Fe^0$-phosphine species,[11,12] formation of ill-defined diamagnetic aggregates stabilized by dmpe ligands is not excluded. Overall, this means that reduced species obtained using Li(hmds) at 80 °C can progressively act as an efficient reservoir of **3**, enabling the C−D activation of $C_6D_6$ affording $\mathbf{4}_{C6D5,D}$, which is not the case when Na(hmds) and K(hmds) are used (entries 11 and 12).

Since a significant mass of iron is not detected by NMR speciation, $^{57}$Fe Mössbauer spectroscopy of the reaction medium was also performed in the same conditions (treatment of $^{57}$**Fe-1** by 10 equiv of Li(hmds) in $C_6D_6$/THF (9:1) at 80 °C during 22 h, followed by 10 h at 20 °C, Figure 1c). The resulting spectrum could be simulated taking into account the presence of four different iron species. Complex $\mathbf{5}^-$ was detected with Mössbauer parameters analogous to previous reports ($\delta$ = 0.57 mm/s, $|\Delta E_Q|$= 0.60 mm/s, green component), accounting for ca. 15% of the overall iron in solution in line with the NMR speciation (Table 1, entry 10).[17b] The major species observed by Mössbauer represents ca. 45% of the overall iron quantity ($\delta$ = 0.19 mm/s, $|\Delta E_Q|$= 0.57 mm/s, Figure 1c, blue line), which is in fair agreement with the amount of $\mathbf{4}_{C6D5,D}$ observed by $^{31}$P NMR speciation (38%). The nuclear parameters of this species are moreover also in agreement with what can be expected from low-spin $Fe^{II}$ hydride species.[23] The broadness of this signal might be due to the existence of both *cis* and *trans* isomers of $\mathbf{4}_{C6D5,D}$, which overall lead to the superposition of two doublets with close parameters. Slight differences in Mössbauer parameters may indeed be expected for the signals of a *cis*/*trans* isomeric pair, as reported by Herber and Hayter.[23c] Moreover, a third, rather broad signal accounting for 35% of the iron speciation displays parameters consistent with low-spin, $Fe^0$ species ($\delta$ = 0.20 mm/s, $|\Delta E_Q|$ = 1.13 mm/s, magenta component).[23a] Formation of such a diamagnetic compound is also in line with the $^{31}$P NMR speciation given in Table 1 and Figure S33, which shows that several ill-defined P-ligated diamagnetic compounds as well as ca. 10% of **3*** are formed. Thus, it is likely that several low-spin $Fe^0$ species, including **3***, may all contribute to the same Mössbauer signal. Last minor unidentified species ($\delta$ = 0.18 mm/s, $|\Delta E_Q|$ = 1.92 mm/s, 5% of the total Fe, cyan component) has also been included in order to obtain the best fit to the experimental spectrum. Overall, both Mössbauer and NMR speciations point toward the formation of $\mathbf{5}^-$, $\mathbf{4}_{C6D5,D}$, and a distribution of diamagnetic P-ligated $Fe^0$ species upon treatment of **1** by Li(hmds) at 80 °C during 22 h, those species accounting for more than 90% of the iron quantity according to the Mössbauer simulation.

This section shows that $C_6D_6$ activation by oxidative insertion of in situ generated $Fe^0$ species upon treatment of **1** by M(hmds) (M = Li, Na, K) is amenable under photolytic conditions and under thermal activation for M = Li.

## Formation of Ar−$Fe^{II}$ Bonds by Deprotonative Ferration

In addition to the detection of $Fe^0$ complexes (which can yield $\mathbf{4}_{C6D5,D}$) that has been described in the previous section, formation of a small amount of $\mathbf{2}_{C6D5}$ (Table 1, entry 8) obtained by combination of **1**, $C_6D_6$, and Na(hmds) also suggests that deprotonative ferration can be reached with the **1**/M(hmds) system. Given that conditions discussed in Table 1 mostly led to easy reduction of **1** with Na(hmds) and K(hmds), the reactivity of Li(hmds) was more closely investigated. **1** was then subjected to treatment by 2 equiv of Li(hmds) in the presence of crown-ether 15-C-5.[24] It was anticipated that quenching of the $Li^I$ cation by 15-C-5 would lead to an enhancement of the hmds anion basicity, thus favoring the C−D bond deprotonation.

When **1** is treated by 2 equiv of Li(hmds) associated with 2 equiv of 15-C-5 at 20 °C during 72 h, reduction into **3′** and **3″** is observed (25% overall, Table 2, entry 1). Deprotonation of


https://doi.org/10.1021/jacsau.3c00649
JACS Au 2024, 4, 512−524

**Table 2. Speciation of Complexes 1−5 Obtained by Treatment of 1 by 2 equiv of Li(hmds) in the Presence or the Absence of 2 equiv of 15-C-5 under Various Conditions**

| entry | M ($n$), additives | $t$ (h) | $T$ (°C) | solvent | light | **1** | $\mathbf{2}_{C6D5}$ | **3′** | **3″** | $Fe_x^0(P,P)_y$ | $\mathbf{4}_{C6D5,D}$ | $\mathbf{5}^-$ |
|---|---|---|---|---|---|---|---|---|---|---|---|---|
| 1 | Li (2), 2 equiv 15-C-5 | 72 | 20 | $C_6D_6$ | no | 50 | 10 | 25% overall[a] | | 0 | 0 | 5 |
| 2 | | 72 | 20 | $C_6D_6$ | yes | 40 | 14 | 0 | 0 | 0 | 40[b] | 0 |
| 3 | | 22 | 80 | $C_6D_6$ | no | 60 | 34 | 0 | 0 | 5 | 0 | traces |
| 4 | Li (2), no 15-C-5 | 22 | 80 | $C_6D_6$ | no | 10 | 0 | 0 | 0 | 30 | 0 | traces |

[a]8% **3*** were observed. [b]Mixture of *cis*:*trans*-$\mathbf{4}_{C6D5,D}$ in a ca. 4:3 ratio.

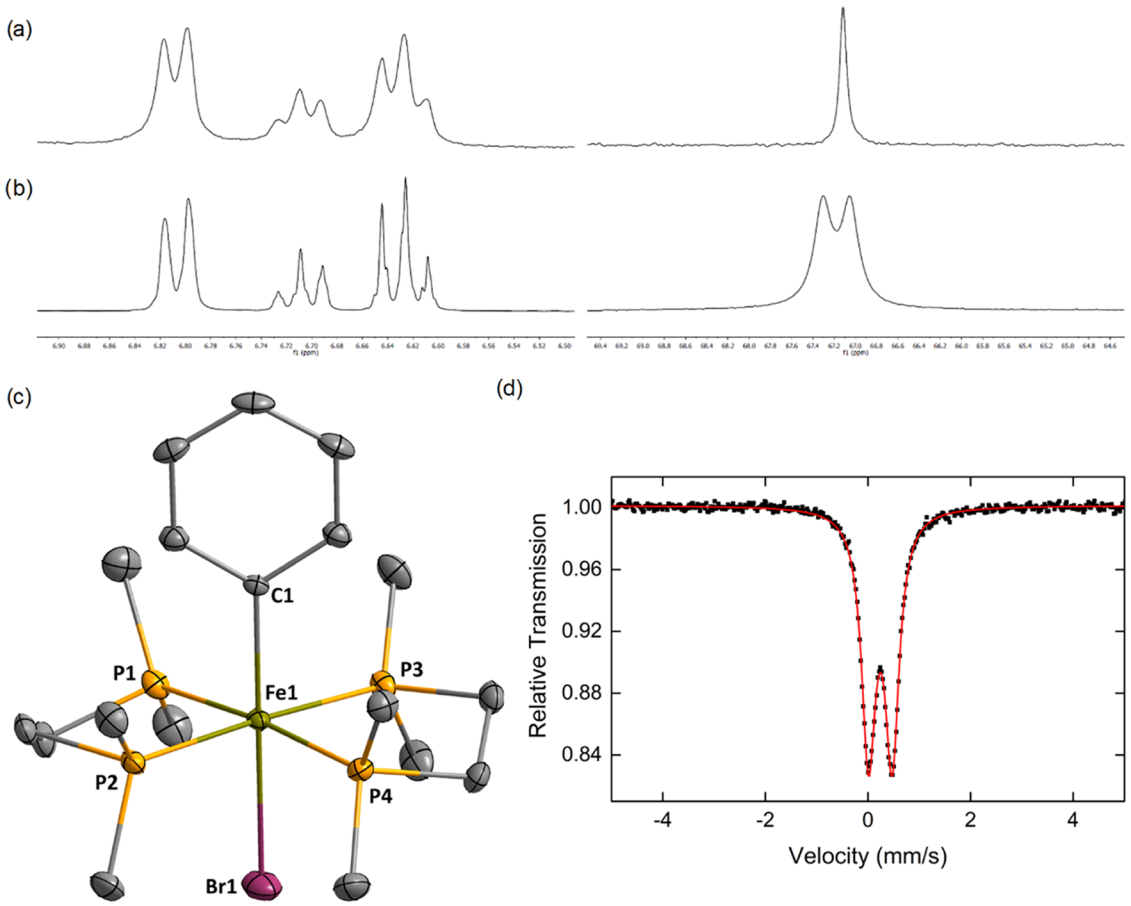


**Figure 2.** $^1$H (left) and $^{31}$P (right) NMR spectra of complexes $\mathbf{2}_{Ph}'$ (a) and $^{57}$**Fe-2**$_{Ph}'$ (b) generated by addition of 1 equiv of PhMgBr (1 M in THF) onto **1** and $^{57}$**Fe-1**; see Figures S3−S8 for full spectra; (c) crystal structure of $\mathbf{2}_{Ph}'$ (hydrogen atoms omitted for clarity, ellipsoids drawn at the 30% probability level); (d) 80 K $^{57}$Fe Mössbauer spectrum of a frozen $C_6D_6$/THF (9:1) solution of $^{57}$**Fe-2**$_{Ph}'$ formed by addition of PhMgBr onto $^{57}$**Fe-1**, with $\delta$ = 0.24 mm/s and $|\Delta E_Q|$ = 0.46 mm/s.

the $C_6D_5$−D bond also occurs as a side pathway, and 10% $\mathbf{2}_{C6D5}$ are detected. Under photolytic conditions (entry 2), 40% of $\mathbf{4}_{C6D5,D}$ are detected, and the quantity of $\mathbf{2}_{C6D5}$ remains roughly unchanged (14%). In line with the results discussed in Table 1 (comparison between entries 2−3 and 5−6), **3′** and **3″** are not observed upon irradiation: it is not excluded that they are formed under photolytic conditions and that their evolution toward **3** and, ultimately, to $\mathbf{4}_{C6D5,D}$ is triggered by light. However, under thermal activation (80 °C, entry 3), $\mathbf{2}_{C6D5}$ was detected (34%) along with unreacted **1** (60%), and small amounts of ill-defined P-ligated diamagnetic species were detected (ca. 5% $Fe_x^0(P,P)_y$, 50−60 ppm area in $^{31}$P NMR, see Figure S36). This means that deprotonation of the $C_6D_5$−D bond by Li(hmds) can be achieved while limiting the reduction in the presence of 15-C-5 under thermal conditions. In the absence of crown-ether at 80 °C (Table 2, entry 4), 90% conversion of **1** is observed. $\mathbf{2}_{C6D5}$ is not detected, and reduced ill-defined diamagnetic $Fe_x^0(P,P)_y$ species are formed (ca. 30% according to $^{31}$P NMR speciation, see Figure S37).[25] In other words, it means that quenching the acidity of the $Li^I$ cation does not preclude formation of $\mathbf{2}_{C6D5}$, but it seems to enhance its stability at 80 °C.

In order to further analyze the reactivity of $\mathbf{2}_{C6D5}$, its brominated analogue $PhFe^{II}(Br)(dmpe)_2$ ($\mathbf{2}_{Ph}'$) was synthesized by anion metathesis between **1** and PhMgBr and isolated.[26] $^{31}$P NMR analysis shows that signatures of $\mathbf{2}_{Ph}'$ and $\mathbf{2}_{C6D5}$ are close ($\delta$ = 67 ppm for both, see Figures 2a and S3−S4 for $^{31}$P and $^1$H NMR spectra of $\mathbf{2}_{Ph}'$ and Figure S36 for $\mathbf{2}_{C6D5}$). Use of labeled $^{57}$**Fe-1** showed unambiguously that $^{57}$**Fe-2**$_{Ph}'$ features a $^{57}$Fe-ligated phenyl anion $C_6H_5^-$, characteristic $^{31}$P−$^{57}$Fe and $^1H_{Ar}$−$^{57}$Fe couplings being


https://doi.org/10.1021/jacsau.3c00649
JACS Au 2024, 4, 512−524

**Scheme 2. Reactivity of Isolated $2_{Ph}'$ (a) or In Situ Generated $2_{C6D5}$ (b) in the Presence of $Li^I$ Salts; X = Br, OTf**

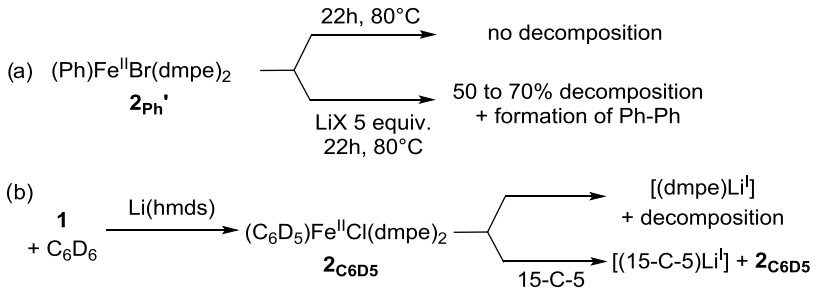


observed ($J(^{31}P-^{57}Fe)$ = 42 Hz; $J(^1H_{meta}-^{57}Fe)$ = 4 Hz; $J(^1H_{para}-^{57}Fe)$ = 3 Hz; see Figure 2b).

Single crystals of $2_{Ph}'$ suitable for X-ray diffraction analysis were obtained by cooling down a $C_6H_6$/THF (9:1) solution layered with pentane at −35 °C during 16 h (Figure 2c). Characterization of this structure by X-ray diffraction completes the NMR description of $2_{Ph}$ reported by Tolman and Ittel in 1979.[11b] $2_{Ph}'$ is one of the rare examples of well-defined structurally characterized low-spin aryliron species in an octahedral environment, with a $C_{ipso}$−Fe distance of 2.08 Å. Camadanli described the formation of low-spin hydrido aryliron(II) species by insertion of $Fe^0(PMe_3)_4$ into the *ortho* C−H bond of an aromatic ketimine, where the C═N bond acts as a directing group.[13] In those species, the $C_{ipso}$−Fe bond is slightly shorter than in $2_{Ph}'$, probably due to the presence of the intramolecular N−Fe ligation. By comparison, the cyclometalated complex $[(benzamide)(dppe)(Ph)Fe^{II}]^-$ described as a dimer by Neidig and Ackermann and involving a nontethered phenyl anion features Ph−Fe bonds of 2.036/2.039 Å, closer to those of $2_{Ph}'$.[9] The $^{57}$Fe Mössbauer spectrum of $^{57}$**Fe-2**$_{Ph}'$ was also recorded in a frozen $C_6D_6$/THF (9:1) solution (Figure 2d). The observed Mössbauer parameters ($\delta$ = 0.24 mm/s and $|\Delta E_Q|$ = 0.46 mm/s) are consistent with a low-spin $Fe^{II}$ center (diamagnetic, $S$ = 0). Similar parameters were reported by Neidig and Gutierrez for the formation of an octahedral aryliron(II) complex featuring depe ligands (depe = 1,2-bis-diethylphosphinoethane), although no X-ray structure was reported for this species.[27]

We then investigated the fate of $2_{Ph}'$ in the presence of $Li^I$ salts such as LiBr or LiOTf. When $2_{Ph}'$ was treated by 5 equiv of those salts in neat $C_6D_6$, degradation of respectively 70 and 50% of $2_{Ph}'$ was observed after 22 h at 80 °C, along with an insoluble dark precipitate. Concomitant formation of Ph−Ph was confirmed by GC-MS, attesting to a reduction of the $Fe^{II}$ ion from $2_{Ph}'$. On the other hand, $2_{Ph}'$ remained unreacted in the absence of $Li^I$ salts under the same conditions (Scheme 2a). Those results demonstrate that $2_{Ph}'$ is thermally stable in the absence of a Lewis-acidic cation, explaining the persistence at 80 °C of its analogue $2_{C6D5}$ when $Li^I$ cation acidity is quenched in the presence of 15-C-5 (Table 2, entry 3).

Decomposition of $2_{Ph}'$ in the presence of $Li^I$ salts into unidentified reduced iron species points toward an interaction of the lithium cation with the iron coordination sphere prior to the reduction. When **1** is treated by Li(hmds) at 80 °C during 22 h (conditions of Table 1, entry 10), a broad distribution in the −49/−50 ppm area is also observed in $^{31}$P NMR (Figure 3a). This is diagnostic of the release of free dmpe in the reaction medium, along with various adducts formed between the latter and $Li^I$ salts, e.g., [dmpe·Li(Y)] (Y = Cl, hmds). $\sigma$-Ligation of $Li^I$ cations by phosphines indeed leads to a minor

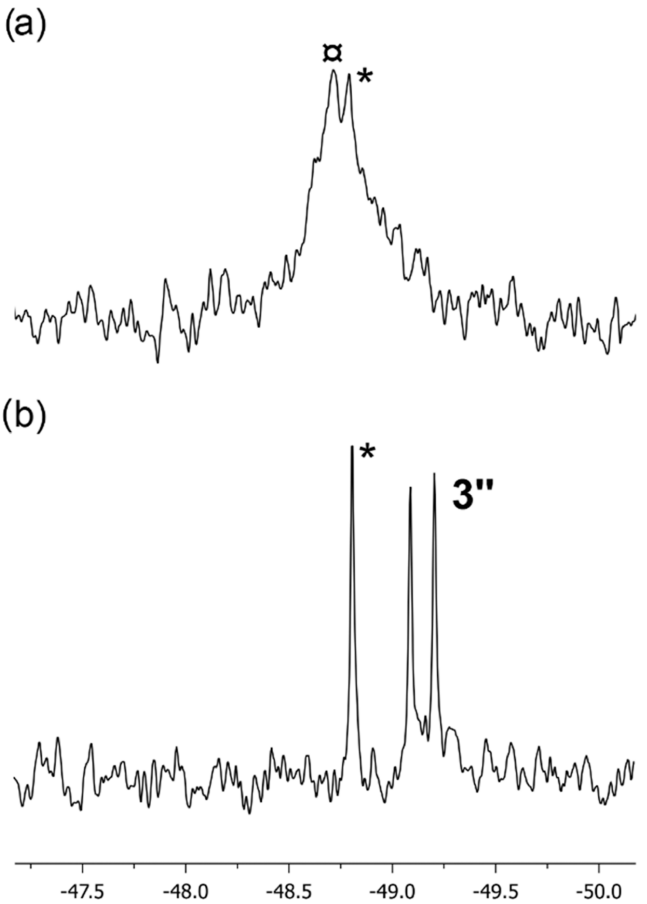


**Figure 3.** $^{31}P\{^1H\}$ NMR spectrum ($C_6D_6$/THF (9:1), 20 °C, restricted to the free dmpe area) of a solution of **1** treated by 10 equiv of M(hmds) after 22 h at 80 °C; M = (a) Li; (b) Na; * = free dmpe, ¤ = [dmpe·$Li^I$] adducts; see Figures S27−S32 for the full spectra.

shift of the latter in $^{31}$P NMR, as reported by Lappert and Layh,[28a] or more recently by Reid for the $Li(dmpe)_3^+$ cation ($\delta(^{31}P)$ = −45.9 ppm in toluene-$d_8$).[28b]

The instability of $2_{Ph}'$ in the presence of $Li^I$ salts (Scheme 2a) and the observation of dmpe-lithium adducts upon treatment of **1** by Li(hmds) (Figure 3a) attest to the demetallating power of the $Li^I$ cation, able to decoordinate the dmpe from the iron. As summarized in Scheme 2b, consumption of $2_{C6D5}$ in the absence of 15-C-5 suggests that the former readily undergoes a demetalation by $Li^I$ cations, affording [dmpe·$Li^I$] adducts along with NMR-silent species. Conversely, trapping the $Li^I$ cation by 15-C-5 prevents demetalation of dmpe from iron, enhancing stability of $2_{C6D5}$ even at 80 °C. No [dmpe·$M^I$] adducts are observed using the


https://doi.org/10.1021/jacsau.3c00649
JACS Au 2024, 4, 512−524

Na/K hmds salts, in agreement with their weaker coordinating properties (Figure 3b). This observation is also in line with the strength of the $Na^{I}$−P ligation described by Reid in the case of the 1,2-bis-dimethylphosphinobenzene (diphos) ligand, much weaker than that of the $Li^{I}$−P analogues (discussion based on the comparison of the metric parameters of the X-ray structure of the $[M(diphos)_3]^+$ adducts; M = Li, Na).[28b] The interaction observed between the $Li^{I}$ cation and the dmpe ligand in the system discussed herein is also in line with other reports from the recent literature. This again demonstrates the crucial role of main-group cations in the evolution of a distribution of organotransition species.[29] Bedford also reported a similar reactivity of $Zn^{II}$ cations in Negishi couplings catalyzed by various (P,P)$Fe^{II}$ salts, where Zn-(P,P) ligation is a key step of the catalytic cycle.[30]

Association of **1** with alkali bases M(hmds) (M = Li, Na, or K) thus affords a simple platform, which unlocks the access to both deprotonative (nonredox) and oxidative ferrations (Scheme 1c, paths (i) and (ii)). The nature of the preferred path is impacted by the alkali countercation. Under thermal activation, K(hmds) promotes formation of reduced species, affording $\mathbf{4}_{C6D5,D}$ by oxidative insertion of **3** into $C_6D_6$, and Na(hmds) allows detection of both $\mathbf{2}_{C6D5}$ and $\mathbf{4}_{C6D5,D}$ intermediates. While treatment of **1** by Na(hmds) and K(hmds) mostly affords silent species (probably reduced aggregates), use of Li(hmds) can lead to either deprotonative ferration (formation of $\mathbf{2}_{C6D5}$) under thermal conditions or $\mathbf{4}_{C6D5,D}$ under harsher conditions. Reduction of **1** followed by C−D activation yielding $\mathbf{4}_{C6D5,D}$ is however observed for M = Li, Na and K under photolytic activation.

Possible catalytic applications of this divergent ferration system are discussed in the next section of this article, with a focus on the cross-coupling, reductive dehydrocoupling, and hydrogen isotopic exchange (HIE) chemistry.

## Reactivity in Cross- and Dehydrogenative Coupling as well as in HIE Chemistry

### Cross-Coupling of Arenes with Organic Electrophiles.

The possible generation of Ar−$Fe^{II}$ compounds such as $\mathbf{2}_{C6D5}$ from **1** by deprotonation of an Ar−H pro-nucleophile with M(hmds) (M = Li, Na) invited us to investigate the possible catalytic applications of this system in cross-coupling transformations. As outlined in the introduction of this report, organoiron(II) species are indeed key intermediates in cross-coupling processes; they are moreover known for efficiently activating aliphatic electrophiles by single electron transfers (SETs).[31] The cross-coupling of $C_6H_6$ with *n*-$C_{12}H_{25}I$ in the presence of 0.1 equiv of **1** and M(hmds) (1 equiv vs *n*-$C_{12}H_{25}I$) has been chosen as a benchmark reaction (Table 3); the main byproduct obtained under those conditions was *n*-$C_{12}H_{26}$, formed by reduction of the starting C−I bond.

A first coupling attempt using Li(hmds) as a base at 40 °C during 72 h only led to traces of the coupling product (Table 3, entry 1). Increasing reaction temperature up to 80 °C however afforded a modest 25% coupling yield (entry 2). Owing to the competitive reduction of **1** into **3**, **3′** and **3″**, Na(hmds) was a much less efficient alkali base and afforded Ph-(*n*-$C_{12}H_{25}$) with a poor 7% yield (entry 3). In line with the formation of more reduced iron species in the reaction medium, reduction product *n*-$C_{12}H_{26}$ is obtained with a higher 17% yield. In a similar way, use of K(hmds) only afforded 9% of coupling product (entry 4). Addition of 15-C-5 to Li(hmds) (entry 5) led to a strong decrease of the coupling yield (1%).

**Table 3. Cross-Coupling between $C_6H_6$ and R-I Mediated by 1 in the Presence of M(hmds) (1 equiv); Yields Based on GC-MS Analysis**

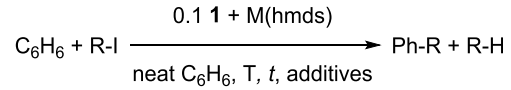


| entry | M | R | T (°C) | t (h) | additives | Ph-R (%) | R-H (%) |
|---|---|---|---|---|---|---|---|
| 1 | Li | *n*-$C_{12}H_{25}$ | 40 | 72 | | 2 | 3 |
| 2 | Li | *n*-$C_{12}H_{25}$ | 80 | 72 | | 25[a] | 10 |
| 3 | Na | *n*-$C_{12}H_{25}$ | 80 | 72 | | 7 | 17 |
| 4 | K | *n*-$C_{12}H_{25}$ | 80 | 72 | | 9 | 9 |
| 5 | Li | *n*-$C_{12}H_{25}$ | 80 | 72 | 15-C-5 20 equiv | 1 | 2 |
| 6[b] | Li | *n*-$C_{12}H_{25}$ | 80 | 72 | | 30[a] | 4 |
| 7[b] | Li | cyclohexyl | 80 | 72 | | 35[a] | n.d. |
| 8[c] | Li | *n*-$C_{12}H_{25}$ | 80 | 72 | | 4 | traces |
| 9 | Li | *n*-$C_{12}H_{25}$ | 80 | 72 | dmpe 1 equiv | 3 | 5 |
| 10 | Li | *n*-$C_{12}H_{25}$ | 80 | 72 | dmpe 3 equiv | 2 | 3 |
| 11[d] | Li | *n*-$C_{12}H_{25}$ | 80 | 72 | | 0 | 0 |
| 12[d] | Li | *n*-$C_{12}H_{25}$ | 80 | 72 | dmpe 1 equiv | 0 | 0 |

[a]Isolated yield. [b]0.1 equiv of $Fe(hmds)_2$ + 1 equiv of dmpe vs Fe; other iron sources. [c]0.1 equiv of $FeCl_2$ [d]No iron source was used.

Since 15-C-5 proved to enhance the stabilization of $\mathbf{2}_{C6D5}$ in the presence of $Li^{I}$ salts (Scheme 2b), this shows that the deprotonation of the Ph−H bond is not the more energetically demanding step of the coupling sequence. Conversely, this demonstrates that the electrophilicity of the $Li^{I}$ cation is requested in the coupling process. Moreover, the best coupling yield (30%, entry 6) is obtained when $Fe^{II}(hmds)_2$ is associated with only 1 equiv of dmpe, evidencing the best performances of unsaturated, single-dmpe coordinated intermediates. Under the same conditions, a similar 35% yield was obtained when iodocyclohexane was used (entry 7). Traces of coupling product are also detected when $FeCl_2$ is used in the absence of dmpe (entry 8). Use of an excess of dmpe is highly detrimental to the reaction outcome, since the coupling yield dropped to 3% (respectively 2%) when 1 equiv of dmpe (respectively 3 equiv) is added to **1** in the reaction medium (entries 9−10, compare with entry 2). Control experiments performed in the absence of iron confirm that the latter is mandatory in the coupling process, since no product is detected when Li(hmds) is used alone or in the presence of dmpe (entries 11−12). At this stage, two possible mechanisms can explain the formation of the C−H coupling product. Either the electrophile is activated by $Fe^{II}$ species such as an arylated complex derived from $\mathbf{2}_{Ph}$, or the formation of a reduced $Fe^{0}$ complex (e.g., **3**, **3′** or **3″**) is required to do so. A stoichiometric experiment was performed, in which reduced iron species are formed by addition of 2 equiv of Li(hmds) on **1** at 80 °C (conditions of Table 2, entry 4), prior to reaction with *n*-$C_{12}H_{25}I$ in the presence of 1 additional equivalent of Li(hmds) (Scheme 3).

In those conditions, 20% of cross-coupling product Ph-(*n*-$C_{12}H_{25}$) are formed, along with 25% *n*-$C_{12}H_{26}$, 7% of 1-dodecene, and 10% *n*-$C_{24}H_{50}$. Those three latter products are formed by reduction of the starting halide *n*-$C_{12}H_{25}I$. In particular, the *n*-$C_{12}H_{26}$/Ph-(*n*-$C_{12}H_{25}$) ratio is much higher in conditions of Scheme 3 (5:4) than in cross-coupling


https://doi.org/10.1021/jacsau.3c00649
JACS Au 2024, 4, 512−524

**Scheme 3. Stoichiometric Experiment for the Cross-Coupling between $C_6H_6$ and $n$-$C_{12}H_{25}I$**

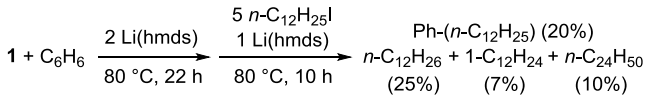


conditions (2:5, Table 3, entry 2). Moreover, 1-dodecene and $n$-$C_{24}H_{50}$ are solely detected as traces in cross-coupling conditions (Table 3, entry 2), whereas they represent 27% of the conversion of $n$-$C_{12}H_{25}I$ in conditions of Scheme 3. This suggests that a sacrificial reduction of $n$-$C_{12}H_{25}I$ occurs when reduced iron species are formed upon treatment of **1** with Li(hmds) and that those species do not contribute to the formation of the coupling product Ph-($n$-$C_{12}H_{25}$). This thus points toward the possible implication of nonreduced $Fe^{II}$ intermediates such as $\mathbf{2_{Ph}}$ or $\mathbf{5}^-$ in the coupling process. Given that the arylated complex $\mathbf{2_{Ph}}$ has been identified as an intermediate on the reduction route of **1** to the $Fe^0$ stage, its reactivity as a coupling intermediate has been further investigated.

The brominated analogue $\mathbf{2_{Ph}}'$ was used as an analytically pure compound, and its treatment by an excess of $n$-$C_{12}H_{25}I$ at 80 °C during 16 h afforded the expected coupling product Ph-($n$-$C_{12}H_{25}$) in a 24% yield (Scheme 4a), demonstrating that $\mathbf{2_{Ph}}'$ is able to promote the coupling step. A similar experiment was performed using $\mathbf{2_{Ph}}'$ generated in situ by transmetalation of PhMgBr with **1** (in conditions of Figure 2, affording a near-quantitative formation of $\mathbf{2_{Ph}}'$ as evidenced by Mössbauer spectroscopy, Figure 2d). This led, after treatment by 10 equiv of $n$-$C_{12}H_{25}I$ in $C_6H_6$, to 43% of coupling product, whereas the coupling yield dropped to 27% in the presence of 15-C-5 (1 equiv vs PhMgBr, Scheme 4b). First, this result importantly demonstrates that the ability of $\mathbf{2_{Ph}}'$ to promote a cross-coupling-type reactivity with $n$-$C_{12}H_{25}I$ is enhanced in the presence of Lewis-acidic cations such as $Mg^{II}$. It is important to note that the Ph-($n$-$C_{12}H_{25}$) yield remains unchanged when thermolysis of $\mathbf{2_{Ph}}'$ is performed in $C_6D_6$ instead of $C_6H_6$ and that only traces of the deuterated compound $C_6D_5$-($n$-$C_{12}H_{25}$) are obtained (Scheme 4b). This confirms that the aromatic core contained in Ph-($n$-$C_{12}H_{25}$) comes from the $Ph^-$ anion bound to the iron. Given that the coupling reactivity of $\mathbf{2_{Ph}}'$ with $n$-$C_{12}H_{25}I$ in the presence of $Mg^{II}$ salts associated with crown-ether 15-C-5 is very close to that of the salt-free, pure complex $\mathbf{2_{Ph}}'$ (respectively 27%, Scheme 4b, and 24%, Scheme 4a), this means that $Mg^{II}$ cations play a key role in the implication of $\mathbf{2_{Ph}}'$ in the catalytic cycle, which is quenched by the presence of the crown-ether. $^{31}P$ NMR monitoring of reaction of a $^{57}\mathbf{Fe\text{-}2_{Ph}}'$ sample (Scheme 4c, top, $\delta$ = 67 ppm, $J(^{31}P-^{57}Fe)$ = 42 Hz), generated in conditions of Figure 2, with 3 equiv of $n$-$C_{12}H_{25}I$ at 80 °C during 4 h also shows that $^{57}\mathbf{Fe\text{-}1}$ and its bromide analogue $^{57}\mathbf{Fe\text{-}1_{Br}}$ are generated in addition to the coupling product Ph-($n$-$C_{12}H_{25}$) (Scheme 4c, bottom, respectively $\delta$ = 59.0 ppm, $J(^{31}P-^{57}Fe)$ = 42 Hz, and $\delta$ = 58.5 ppm, $J(^{31}P-^{57}Fe)$ = 41 Hz). The stoichiometric reactivity of $\mathbf{2_{Ph}}'$ in cross-coupling (Scheme 4a,b) shows without doubt that the presence of a Lewis-acidic cation ($Mg^{II}$ in Scheme 4a,b) plays a beneficial role in the reaction outcome. In line with the observations of adducts such as [dmpe·Li(Y)] by $^{31}P$ NMR (Figure 3a), it can be suggested that $Mg^{II}$ salts enable the decoordination of one dmpe ligand from $\mathbf{2_{Ph}}'$, unlocking the access to unsaturated ferrous species able to promote the cross-coupling. Despite the apparent HSAB

**Scheme 4. Stoichiometric Reactivity of $\mathbf{2_{Ph}}'$[a]**

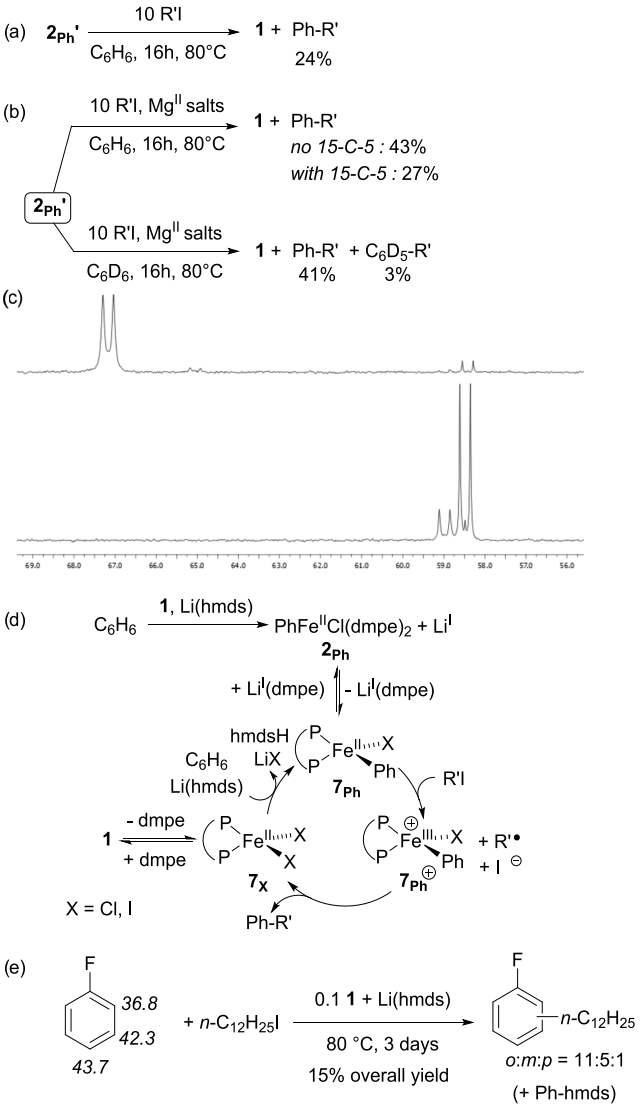


[a]Used either (a) pure or (b) generated by addition of 1 equiv of PhMgBr on **1** followed by 15 h at 20 °C with R′I (R′ = $n$-$C_{12}H_{25}$); (c) $^{31}P$ NMR monitoring of reaction of $^{57}\mathbf{Fe\text{-}2_{Ph}}'$ (top) with 3 equiv of $n$-$C_{12}H_{25}I$ (bottom) during 4 h at 80 °C; (d) plausible catalytic cycle for the cross-coupling of $C_6H_6$ with R′I involving $\mathbf{2_{Ph}}$ as a catalyst reservoir (X = Cl, I); (e) cross-coupling attempt performed on PhF ($pK_a$ of the C−H bonds italicized).

mismatch between the hardness of $Mg^{II}$ ions and softness of P-ligands, weak, labile interaction between $PMe_3$ and $Mg^{II}$ ions in Grignard reagents has already been probed.[32a] Moreover, Arnold also reported an example of structurally characterized $Mg^{II}$ adduct with alkyl 1,2-diphosphines, demonstrating the possible interaction between alkyl phosphines and $Mg^{II}$ salts.[32b]

Since $\mathbf{2_{C6D5}}$ is readily obtained by direct ferration of $C_6D_6$ mediated by Li(hmds) (Table 2, entry 3), this also means that $\mathbf{2_{C6D5}}$ can act as an intermediate in the cross-coupling between $C_6D_6$ and $n$-$C_{12}H_{25}I$. $Li^I$ and $Mg^{II}$ cations can thus act as a dmpe reservoir in a catalytic process: the main role of the dmpe therefore mostly seems to provide a coordination sphere able to stabilize transiently unsaturated Ph−$Fe^{II}$ intermediates toward decomposition pathways, even if decoordination of the


https://doi.org/10.1021/jacsau.3c00649
JACS Au 2024, 4, 512−524

dmpe ligand from the iron center also seems to be mandatory in another step of the coupling cycle.

Those results unambiguously show that the coordination strength of the alkali countercation is a key parameter of the coupling discussed in Table 3. A likely explanation is that $\mathbf{2_{Ph}}$, owing to its octahedral low-spin $d^6$ configuration, also displays a certain inertia toward reaction with $n$-$C_{12}H_{25}I$. The $Li^I$ cation is then prompt to promote the decoordination of one dmpe ligand of $\mathbf{2_{Ph}}$, affording a nonsaturated 14-VE complex $PhFe^{II}(dmpe)Cl$ ($\mathbf{7_{Ph}}$), which will react with the organic electrophile in a SET step to afford $Fe^{III}$ intermediate $\mathbf{7_{Ph}}^+$ (Scheme 4d). Similar trends were reported by Gutierrez and Neidig, who showed that saturated octahedral 18-VE $(P,P)_2Fe^{II}(Ar)X$ proved to be inert in coupling processes, whereas unsaturated tetrahedral 14-VE analogues $(P,P)$-$Fe^{II}(Ar)X$ displayed excellent performances.[27] The requirement of a decoordination of one dmpe ligand during the process is moreover confirmed herein by the detrimental effect of the excess of dmpe on the reaction outcome (Table 3, entries 9−10, to be compared with entry 2). An outer-sphere radical recombination between $\mathbf{7_{Ph}}^+$ and $n$-$C_{12}H_{25}^{\bullet}$ then affords the coupling product Ph-($n$-$C_{12}H_{25}$) with $\mathbf{7_X}$, as observed in classic aryl-alkyl Fe-catalyzed couplings (Scheme 4d).[31] $\mathbf{7_X}$ (in equilibrium with $\mathbf{1}$, as evidenced in Scheme 4c) finally re-enters the catalytic cycle after deprotonation of another equivalent of benzene. The proficiency of a SET/radical recombination sequence as key steps has been probed by the coupling of $C_6H_6$ with 1-bromohexene as a radical clock, which selectively afforded cyclization product $PhCH_2C_5H_9$ (see Section S4b). It is also not excluded that a dmpe-free intermediate such as $Fe^{II}(hmds)_3^-$ ($\mathbf{5}^-$, evidenced by $^1H$ NMR and Mössbauer speciations, see Table 1, entry 10 and Figure 1c) also initiates a catalytic cycle with deprotonation of $C_6H_6$, leading to a dmpe-free Ph-$Fe^{II}$ compound. The latter would react in a SET step with the electrophile, since traces of cross-coupling product are also observed when $FeCl_2$ is used as an iron precursor in the absence of dmpe (Table 3, entry 8). This would be in line with the reducing activity of similar ferrate species such as $[Me_3Fe^{II}]^-$, which was reported by Uchiyama, those *ate* complexes proving to readily undergo single-electron oxidation by a variety of electrophiles.[33] In our case, the poor amount of cross-coupling product obtained in the absence of dmpe however suggests that the latter is required to stabilize on-cycle, undercoordinated intermediates.

As detailed above, formation of $\mathbf{2_{Ph}}'$ under coupling relevant conditions and ability of the latter to provide the expected cross-coupling product Ph-($n$-$C_{12}H_{25}$) by reaction with $n$-$C_{12}H_{25}I$ (Scheme 4a−c) suggests that metalation of the Ar−H bond occurs prior to formation of the radical $n$-$C_{12}H_{25}^{\bullet}$. An alternative mechanism would be the formation of $n$-$C_{12}H_{25}^{\bullet}$ followed by addition of the latter onto $C_6H_6$ in a radical nucleophilic addition mechanism. In this alternative mechanism, a C−H bond then undergoes homolytic cleavage to restore the aromaticity. In order to decipher whether the coupling step may also proceed following this alternative radical-based mechanism, a cross-coupling attempt has been performed using fluorobenzene (PhF) as a C−H bond source in the conditions of Table 3, entry 2 ($n$-$C_{12}H_{25}I$ treated by 0.1 equiv of $\mathbf{1}$ and 1 equiv of Li(hmds) in neat PhF at 80 °C during 3 days). PhF has been chosen as a mechanistic probe since it can be activated by both the deprotonative pathway and radical addition mechanism;[34] it moreover displays three C−H bonds with very distinct acidities ($pK_{a(ortho\ H)}$ = 36.8, $pK_{a(meta\ H)}$ = 42.3, $pK_{a(para\ H)}$ = 43.7, Scheme 4e).[34a] Cross-coupling of PhF with $n$-$C_{12}H_{25}I$ in the presence of Li(hmds) (1 equiv per mole of electrophile) led to a poor 15% yield in coupling products, significant quantities of Ph-$N(SiMe_3)_2$ being formed by defluorination of the starting material. A 11:5:1 distribution of the *ortho*/*meta*/*para* isomers of the cross-coupled product $C_6H_4F$($n$-$C_{12}H_{25}$) is observed. This distribution can be indicative of the proficiency of a radical-based mechanism, since it is very similar to the 11.2:7.6:1 ratio reported in such conditions under Pd-catalyzed addition of alkyl radicals onto PhF.[34b] In a pure deprotonative mechanism, an almost exclusive metalation at the *ortho* position would be expected, in line with the ability of PhF to undergo this process.[34c] Therefore, taken together, those results demonstrate that some part of the coupling activity can also be attributed to a radical-based mechanism, in addition to the deprotonative way discussed earlier and involving the intermediate $\mathbf{2_{Ph}}$. This would explain the detection of traces of $C_6D_5$-($n$-$C_{12}H_{25}$) as a coupling product when $C_6D_6$ is used as a solvent in the thermolysis of $\mathbf{2_{Ph}}'$ (Scheme 4b). $\mathbf{2_{Ph}}'$ would thus undergo oxidation by SET with $n$-$C_{12}H_{25}I$, but $C_6D_5$-($n$-$C_{12}H_{25}$) would be formed by addition of the $n$-$C_{12}H_{25}^{\bullet}$ radical onto $C_6D_6$, bypassing its recombination with the iron-bound $C_6H_5$ group. In this radical mechanism, it is not excluded that nonarylated species such as $Fe^{II}(hmds)_3^-$ ($\mathbf{5}^-$) also act as one-electron reductants. However, it is also possible that the nature of the preferred mechanism (deprotonative way or radical addition) also depends on the Ar−H target.

**C−H/B−H Bond Metathesis: Reductive Dehydrocoupling.** Given that formation of elusive species $\mathbf{3}$ proved to occur upon reduction of $\mathbf{1}$ with Li, Na, and K hmds salts under photochemical activation, leading to $\mathbf{3}'$, $\mathbf{3}''$, or $\mathbf{4_{C6D5,D}}$ (Table 1, entries 4−6), we also aimed at exploring potential catalytic applications of this system. As outlined in the introduction of this report, formation of hydrido aryliron species $\mathbf{4_{Ar,H}}$ (Scheme 1b) is a key step in various transformations such as reductive dehydrocoupling. It was for example reported in 2015 that borylation of $C_{Ar}$−H bonds could be performed by photolytic generation of $\mathbf{3}$ from $Fe^{II}(R)_2(dmpe)_2$ (R = H, Me) in good to moderate yields.[12a] Performances of $\mathbf{1}$ associated with M(hmds) (M = Li, Na, K) in the reductive dehydrocoupling of $C_6D_6$ and pinacolborane pinBH, leading to formation of perdeuterophenyl pinacolborane $C_6D_5$-B(pin), were then investigated (Table 4). The transformation was monitored at room temperature by multinuclear NMR analysis ($^{31}P$, $^{11}B$, $^1H$). No borylation product $C_6D_5$-B(pin) was detected after 3 days when $\mathbf{1}$ was treated by 2 equiv of Na(hmds) in $C_6D_6$ in the presence of 10 equiv pinBH per mole of Fe (Table 4, entry 1). Under those conditions, no reduction of $\mathbf{1}$ and no further evolution to $\mathbf{4_{C6D5,D}}$ were observed. To circumvent this matter, $\mathbf{1}$ was treated with 2 equiv of Na(hmds) during 72 h prior to addition of pinBH, affording the expected distribution of $\mathbf{3}$, $\mathbf{3}'$, and $\mathbf{4_{C6D5,D}}$ species as detailed in the previous section (see the SI). After addition of pinBH, no evolution was observed after 7 days at 20 °C when the medium was kept in darkness (entry 2). However, upon irradiation at 365 nm, $^{11}B$ NMR monitoring showed progressive formation of $C_6D_5$-B(pin) ($\delta$ = 31.3 ppm, see the SI), see entry 3. A 15% borylation yield (respectively 30%) was observed after 72 h (respectively 6 days). After 10 days, 35% of $C_6D_5$-B(pin) were formed, with an overall incomplete 80% pinBH conversion, suggesting a deactivation of the catalyst. Interestingly, substitution of Na(hmds) by Li(hmds) led to a


https://doi.org/10.1021/jacsau.3c00649
JACS Au 2024, 4, 512−524

**Table 4. Borylation of $C_6D_6$ by pinBH and Deuteration of pinBH Mediated by 1 in the Presence of M(hmds) (M = Li, Na, K) under Photochemical Activation (in $C_6D_6$/THF 9:1)[a]**

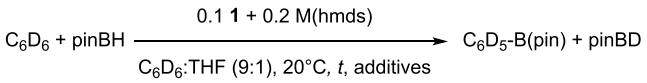


| entry | M | $t$ (days) | conditions | $C_6D_5$–B(pin) | pinBD | pinBH |
|---|---|---|---|---|---|---|
| 1 | Na | 3 | no light | 0 | 0 | 100 |
| 2 | Na | 7 | no light[b] | 0 | 0 | 100 |
| 3 | Na | 3 | $h\nu$[b] | 15 | 17 | 66 |
| | | 6 | | 30 | 30 | 29 |
| | | 10 | | 35 | 35 | 21 |
| 4 | Li | 3 | $h\nu$[b] | 75 | 8 | 6 |
| | | 4 | | 80 | 4 | 3 |
| | | 6 | | 87 (60)[c] | 0 | 0 |
| 5 | K | 4 | $h\nu$[b] | 5 | <5 | 88 |
| | | 10 | | 15 | 15 | 60 |

[a] $^{11}$B NMR yields are given. [b] Premix of M(hmds) with **1** (72 h) prior to addition of pinBH; see Figures S56–S58 for $^{11}$B NMR monitoring. [c] Isolated yield.

much more efficient conversion, since 75% of $C_6D_5$–B(pin) are formed after 3 days (entry 4). Progressive consumption of pinBH leads to a 80% borylation yield after 4 days; no starting material is detected after 6 days, with a 87% $C_6D_5$–B(pin) yield (isolated yield: 60%). The isolated yield obtained using this method is moreover higher than that was reported using the more sensitive precursor $Fe^{II}(Me)_2(dmpe)_2$ (34% PhB-(pin) after 3 days[12a]). K(hmds) led to a poor 15% borylation yield after 10 days and an incomplete 40% conversion, also suggesting a catalyst deactivation (entry 5).

The slow but complete evolution of the pinBH conversion using Li(hmds) as a reductant of **1** under irradiation clearly demonstrates that in situ generated active species **3** does not decompose over time, whereas catalyst deactivation is observed with Na(hmds) and especially with K(hmds). A possible explanation is that Na(hmds) and K(hmds) have a too strong reducing power, leading to higher concentrations of $Fe^0$ species (such as **3**, **3′**, and **3″**) and hence to decomposition of the latter over time by formation of unreactive metallic aggregates, leading overall to poorer catalytic activities. In line with this remark, significant quantities of unreacted **1** are observed by $^{31}$P NMR monitoring (Figures S48, S51, S54) of the reaction medium during catalysis when Li(hmds) is used as a precursor; a smaller quantity of **1** is detected when Na(hmds) is used, and only traces of **1** are detected for K(hmds), in line with the increasing reducing ability of the M(hmds) salts in the Li/Na/K series. Owing to the less strong reducing power of Li(hmds), the dynamic concentration of transient $Fe^0$ species in the reduction course of **1** with Li(hmds) would then remain low enough to prevent their aggregation. $^{31}$P NMR monitoring shows that complexes $\mathbf{4_{C6D5,D}}$, $Fe^{II}(H)_2(dmpe)_2$ along with $Fe^{II}(H)(D)(dmpe)_2$ ($\delta$ = 76.7 (triplet) and 67.1 (triplet) ppm,[12a]) are formed during the photolyses with Li, Na, and K hmds salts, which attests to the feasibility of the C–D and B–H bond activations by oxidative additions of **3** in this catalytic system. Formation of $H_2$ and of its isotopologue H–D is also confirmed by $^1$H NMR (Figure S52), also attesting to the proficiency of the C–D and B–H bond activations in the dehydrocoupling process (Scheme 5, cycle (i)). Those species are not detected in the absence of irradiation. Moreover, pinBD is also detected by $^{11}$B NMR during the photolysis with a diagnostic signal at $\delta$ = 28.4 ppm (triplet, $^1J(^{11}B–^2D)$ = 21 Hz), regardless of the nature of the M(hmds) cation (Table 4). This is also in line with the known reactivity of **3** in $C_{Ar}$–H and B–H bond activations.[12a]

In the recent literature, pinacolborane has been clasically associated with several nucleophilic partners such as *t*BuONa to efficiently reduce divalent transition-metal complexes L[$M^{II}$] of the third row (L = P- or N-based pincers and M = Fe, Co).[35] In those cases, *t*BuONa acts as a "masked reducing agent", enabling formation of [pinB(O*t*Bu)-(H)]$^-$;$Na^+$, which itself allows the reduction of the [$M^{II}$] complex. It is thus not excluded that this mechanism also contributes to the generation of the active $Fe^0$ species in the case discussed herein, additionally to the direct reduction of **1** under irradiation as evidenced by speciation in Table 1. However, since no reduction of **1** by Na(hmds) was observed in the presence of pinBH (Table 4, entry 1), a reduction mechanism relying on boron hydrides seems unlikely in the case of the Na(hmds). More importantly, the outcome of the transformation is also strongly impacted by the nature of the M(hmds) cation. As discussed earlier, Li(hmds) indeed allows a full conversion of pinBH, yielding 87% of $C_6D_5$–B(pin) (Table 4, entry 4), whereas Na(hmds) affords a modest 35% yield (entry 3). In the former case, a fast C–D/B–H $\sigma$-bond metathesis is observed (Scheme 5, cycle (ii)). However, both pinBD and pinBH are consumed by the borylation path (entry 4, and Scheme 5, cycle (i)), leading to $C_6D_5$–B(pin). On the other hand, when Na(hmds) is used, a progressive increase of

**Scheme 5. Plausible Borylation (i) and C–D/B–H $\sigma$-Bond Metathesis (ii) Cycles Mediated by In Situ Generated 3 in the Presence of M(hmds) (M = Li, Na); (P,P) = dmpe, Ar = $C_6D_5$**

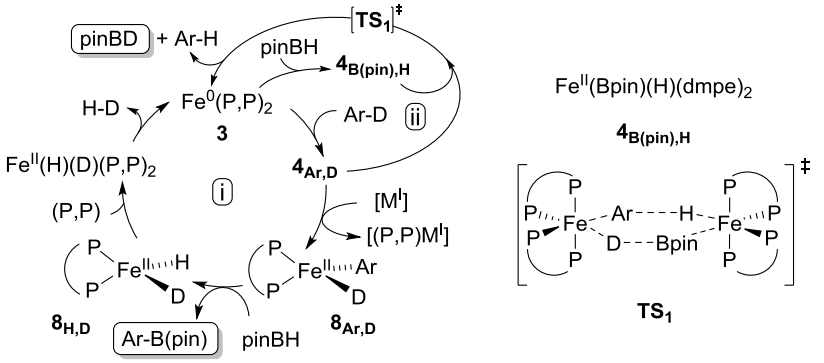




https://doi.org/10.1021/jacsau.3c00649
JACS Au 2024, 4, 512–524

the pinBD yield is observed (up to 35%, entry 3). This suggests that the $C_{Ar}$−B(pin) bond formation path is less operative when Na(hmds) is used instead of Li(hmds), but that the C−D/B−H $\sigma$-bond metathesis path still operates efficiently with Na(hmds).

The nature of the alkali cation can thus govern the reactivity of $\mathbf{4}_{C6D5,D}$, formed after oxidative insertion of **3** into the $C_{Ar}$−D bond (Scheme 5). It has been suggested previously that formation of unsaturated species by loss of at least one arm of a dmpe ligand was involved in the $C_{Ar}$−B bond formation step.[12a] When Li(hmds) is used, this step can be triggered by the demetallating power of $Li^{I}$, leading to unsaturated complex $\mathbf{8}_{C6D5,D}$ (Scheme 5, cycle (i)). Demetalation of one dmpe is also probably triggered by the photoirradiation of the system, which usually leads to a ligand labilization in saturated, inert intermediates, such as low-spin octahedral ferrous complexes. $\mathbf{8}_{C6D5,D}$ affords the borylation product $C_6D_5$−B(pin), along with $\mathbf{8}_{H,D}$. Reintroduction of dmpe in the iron coordination sphere followed by reductive elimination regenerates **3** and affords H−D, detected by $^1$H NMR (Scheme 5, cycle (i)). However, in the presence of Na(hmds), owing to the weak demetallating power of the $Na^{I}$ cation, cycle (i) in Scheme 5 is difficultly followed due to the slow formation of $\mathbf{8}_{C6D5,D}$. Instead, a C−D/B−H $\sigma$-bond metathesis is observed, possibly by reaction between C−D and B−H activated intermediates $\mathbf{4}_{C6D5,D}$ and $\mathbf{4}_{B(pin),H}$ (Scheme 5, cycle (ii)). This ligand scrambling step between two saturated octahedral species might involve a bimetallic transition state ($\mathbf{TS_1}$), as suggested in Scheme 5. The use of Na(hmds), in this case, slows down the demetalation of a dmpe ligand from one of the $Fe^{II}$ ions, enabling the $\sigma$-bond metathesis to occur between those two saturated complexes, overall leading to the formation of pinBD and $C_6D_5H$.

These preliminary results show that **1** can be used as an efficient precursor to induce the formation of $Fe^0$ species such as **3** in a reducing medium leading to activation of $C_{Ar}$−D and B−H bonds under photochemical conditions. More importantly, the judicious choice of the alkali countercation of the reductant, herein M(hmds), can drive the formation of $C_{Ar}$−B bonds by reductive dehydrocoupling (M = Li, Na), or the deuteration of B−H bonds affording B−D species by $\sigma$-bond metathesis can be observed (M = Na). This opens the way to promising synthesis of deuteroboranes $R_2BD$ from boranes $R_2BH$, using $C_6D_6$ as a mild deuterium source and **1** as an easily handled iron catalyst, thus making a sustainable alternative to the classic formation of B−D bonds by addition of borodeuterides such as $NaBD_4$ or $LiAlD_4$ on electrophilic halogenoboranes $R_2BX$. Those methods indeed lead to stoichiometric amounts of salts as byproducts and rely on expensive deuteride sources (molar price of $NaBD_4$ (respectively $LiAlD_4$) being roughly 6 (respectively 30) times higher than that of $C_6D_6$).[36]

## CONCLUSIONS

In this report, we demonstrated that alkali salts M(hmds) can be used as bases or reductants to promote C−Fe bond formations from C−H substrates, respectively, by deprotonative ferration at a $Fe^{II}$ center or by oxidative insertion of transient $Fe^0$ species. These striking differences clearly show that the reactivity of M(hmds) toward $C_6H_6$ and **1** is impacted by the nature of the alkali countercation $M^+$. Depending on the latter, $hmds^-$ can act as a base and follow a nonredox ferration path affording Ar−$Fe^{II}$ species able to react with organic halides in a cross-coupling process (M = Li). On the other hand, $hmds^-$ can also act as a two-electron reductant of **1**, affording elusive species $Fe^0(dmpe)_2$ and promoting C−H insertion reactions leading to heteroleptic Ar−$Fe^{II}$−H intermediates (M = Li, Na, K). Under photolytic activation, this path can be efficiently used to promote either the catalytic borylation of arenes (the best yield and selectivity being afforded by M = Li) or the deuteration of boranes $R_2BH$ using $C_6D_6$ as a deuterium source by $\sigma$-bond metathesis (being observed for M = Na, along with borylation). In all cases, the coordinating properties of the alkali cation $M^+$ can govern the evolution of the iron complex distribution, playing a crucial role in the control of the oxidation state of the latter species as well as of their coordination sphere. Those countercations are thus far from being mere spectators in the catalytic transformations discussed herein and strongly contribute to the generation of the key on-cycle species from their inert resting states. This report thus also provides another example of the crucial importance of alkali cations in organometallic catalysis, which have long proved to strongly contribute to the selectivity of a large variety of transformations.[37]

## METHODS

### Materials and Reagents

All the samples were prepared in a Jacomex Campus glovebox under an argon atmosphere or vacuum Schlenk lines. Glassware equipped with a J. Young valve was dried overnight at 120 °C before use. Deuterated solvents purchased from Eurisotop were thoroughly degassed by freeze−thaw cycles and dried overnight on 4 Å molecular sieves. Nondeuterated solvents were dried over a Na/benzophenone mixture and distilled before use. NMR tubes equipped with a J. Young valve were used for all NMR experiments. Chemicals were obtained from commercial sources and used as purchased, unless specified otherwise or after drying when necessary. A Thorlabs' M365LP1 LED (nominal wavelength = 365 nm, fwhm = 9 nm) mounted to the end of a 57 mm heat sink enabling heat dissipation has been used for the irradiation setup. The details of the synthetic procedures to prepare both iron complexes, $Fe(Cl)_2(dmpe)_2$ (**1**) and $FeBr(C_6H_5)(dmpe)_2$ ($\mathbf{2_{Ph}'}$), are described in the Supporting Information.

### General Procedure for Cross-Coupling Reactions

The reaction with $Fe(Cl)_2(dmpe)_2$ (**1**) and Li(hmds) at 80 °C is given as an example (Table 3, entry 2). In an argon-filled glovebox, a 12 mL vial equipped with a magnetic stir bar was loaded with $Fe(Cl)_2(dmpe)_2$ (3.5 mg, 8.4 $\mu$mol, 0.1 equiv), $C_6H_6$ (1.5 mL), and decane as an internal standard for GC-MS analysis. The mixture was placed under stirring, and $n$-$C_{12}H_{25}I$ (20.2 $\mu$L, 82 $\mu$mol, 1 equiv) was added dropwise followed by Li(hmds) (15.0 mg, 82 $\mu$mol, 1 equiv). The color of the reaction medium gradually changed from emerald green to yellow/orange. The reaction mixture was stirred for 5 min and transferred into an NMR tube fitted with a J. Young valve. The tube was placed in an oil bath at 80 °C and left for 72 h. The color turned pale yellow. The tube was cooled to room temperature and quenched with 2 mL of $H_2O$. The solution was extracted with 2 mL of MTBE and analyzed by GC-MS.

### General Procedure for Dehydrocoupling Reactions

The reaction with $Fe(Cl)_2(dmpe)_2$ (**1**) and Li(hmds) is given as an example (Table 4, entry 4). In an argon-filled glovebox, a 12 mL vial equipped with a magnetic stir bar was loaded with $Fe(Cl)_2(dmpe)_2$ (3.7 mg, 8.7 $\mu$mol, 0.1 equiv), $C_6D_6$ (0.6 mL), and THF in a 9:1 ratio. The mixture was placed under stirring, and Li(hmds) (2.9 mg, 17.3 $\mu$mol, 0.2 equiv) was added. The color of the reaction medium gradually changed from emerald green to yellow/orange. The reaction mixture was stirred for 3 days at room temperature in order to afford the expected distribution of **3**, **3′**, and $\mathbf{4}_{C6D5,D}$ species, monitored by $^{31}$P NMR. Pinacolborane (12.6 $\mu$L, 87 $\mu$mol, 1 equiv) was added, and


https://doi.org/10.1021/jacsau.3c00649
JACS Au 2024, 4, 512−524

the mixture was transferred into an NMR tube fitted with a J. Young valve. The tube was irradiated, and the reaction was monitored by $^{11}B$, $^{31}P\{^{1}H\}$ and $^{1}H$ NMR.

## ■ ASSOCIATED CONTENT

### Supporting Information

The Supporting Information is available free of charge at https://pubs.acs.org/doi/10.1021/jacsau.3c00649.

vw479_0m (CIF)

General procedures, $^{1}H$, $^{31}P$, $^{11}B$, $^{19}F$ NMR spectra (PDF)

## ■ AUTHOR INFORMATION


### Corresponding Authors

**Michael L. Neidig** − *Inorganic Chemistry Laboratory, Department of Chemistry, University of Oxford, Oxford OX1 3QR, U.K.;* orcid.org/0000-0002-2300-3867; Email: michael.neidig@chem.ox.ac.uk

**Guillaume Lefèvre** − *CNRS, Institute of Chemistry for Life and Health Sciences, CSB2D, Chimie ParisTech, PSL University, 75005 Paris, France;* orcid.org/0000-0001-9409-5861; Email: guillaume.lefevre@chimieparistech.psl.eu

### Authors

**Vincent Wowk** − *CNRS, Institute of Chemistry for Life and Health Sciences, CSB2D, Chimie ParisTech, PSL University, 75005 Paris, France*

**Alexis K. Bauer** − *Department of Chemistry, University of Rochester, Rochester, New York 14627, United States*

**Aleksa Radovic** − *Department of Chemistry, University of Rochester, Rochester, New York 14627, United States*

**Lise-Marie Chamoreau** − *CNRS, Institut Parisien de Chimie Moléculaire, Sorbonne Université, F-75252 Paris, France*

Complete contact information is available at: https://pubs.acs.org/10.1021/jacsau.3c00649


### Author Contributions

The manuscript was written through contributions of all authors. All authors have given approval to the final version of the manuscript.


### Funding

G.L. thanks the ERC (Project DoReMI StG, 852640) and the CNRS (Project IrMaCAR) for their financial support. The NMR shared facilities of Chimie ParisTech (Dr. M.-N. Rager) are thanked for technical support.


### Notes

The authors declare no competing financial interest.

## ■ REFERENCES


(1) Gensch, T.; Hopkinson, M. N.; Glorius, F.; Wencel-Delord, J. Mild metal-catalyzed C−H activation: examples and concepts. *Chem. Soc. Rev.* **2016**, *45*, 2900−2936, DOI: 10.1039/C6CS00075D.

(2) Shang, R.; Ilies, L.; Nakamura, E. Iron-Catalyzed C−H Bond Activation. *Chem. Rev.* **2017**, *117* (13), 9086−9139.

(3) (a) Bauer, I.; Knölker, H.-J. Iron Catalysis in Organic Synthesis. *Chem. Rev.* **2015**, *115*, 3170−3387. (b) Bedford, R. B.; Brenner, P. B. *The Development of Iron Catalysts for Cross-coupling Reactions. Iron Catalysis II*; Bauer, E., Ed.; Springer International, 2015.

(4) (a) Carpenter, S. H.; Neidig, M. L. A Physical-Inorganic Approach for the Elucidation of Active Iron Species and Mechanism in Iron-Catalyzed Cross-Coupling. *Isr. J. Chem.* **2017**, *57*, 1106−1116. (b) Neidig, M. L.; Carpenter, S. H.; Curran, D. J.; DeMuth, J. C.; Fleischauer, V. E.; Iannuzzi, T. E.; Neate, P. G. N.; Sears, J. D.; Wolford, N. J. Development and Evolution of Mechanistic Understanding in Iron-Catalyzed Cross-Coupling. *Acc. Chem. Res.* **2019**, *52* (1), 140−150.

(5) Clémancey, M.; Cantat, T.; Blondin, G.; Latour, J.-M.; Dorlet, P.; Lefèvre, G. Structural Insights into the Nature of $Fe^{0}$ and $Fe^{I}$ Low-Valent Species Obtained upon the Reduction of Iron Salts by Aryl Grignard Reagents. *Inorg. Chem.* **2017**, *56*, 3834−3848.

(6) For recent references by some of us on 2-electron reductive eliminations in Fe-catalyzed couplings, see (a) Rousseau, L.; Herrero, C.; Clémancey, M.; Imberdis, A.; Blondin, G.; Lefèvre, G. Evolution of Ate-Organoiron(II) Species towards Lower Oxidation States: Role of the Steric and Electronic Factors. *Chem. - Eur. J.* **2020**, *26*, 2417−2428. (b) Wowk, V.; Rousseau, L.; Lefèvre, G. Importance of Two-Electron Processes in Fe-Catalyzed Aryl-(hetero)aryl Cross-Couplings: Evidence of $Fe^{0}/Fe^{II}$ Couple Implication. *Organometallics* **2021**, *40* (19), 3253−3266. (c) Zhou, E.; Chourreu, P.; Lefèvre, N.; Ahr, M.; Rousseau, L.; Herrero, C.; Gayon, E.; Cahiez, G.; Lefèvre, G. Mechanistic Facets of the Competition between Cross-Coupling and Homocoupling in Supporting Ligand-Free Iron-Mediated Aryl−Aryl Bond Formations. *ACS Org. Inorg. Au* **2022**, *2* (4), 359−369.

(7) Wunderlich, S. H.; Knochel, P. Preparation of Functionalized Aryl Iron(II) Compounds and a Nickel-Catalyzed Cross-Coupling with Alkyl Halides. *Angew. Chem., Int. Ed.* **2009**, *48*, 9717−9720.

(8) (a) Norinder, J.; Matsumoto, A.; Yoshikai, N.; Nakamura, E. Iron-Catalyzed Direct Arylation through Directed C−H Bond Activation. *J. Am. Chem. Soc.* **2008**, *130* (18), 5858−5859. (b) Doba, T.; Matsubara, T.; Ilies, L.; Shang, R.; Nakamura, E. Homocoupling-free iron-catalysed twofold C−H activation/cross-couplings of aromatics via transient connection of reactants. *Nat. Catal.* **2019**, *2*, 400−406. (c) Doba, T.; Ilies, L.; Sato, W.; Shang, R.; Nakamura, E. Iron-catalysed regioselective thienyl C−H/C−H coupling. *Nat. Catal.* **2021**, *4*, 631−638. (d) Doba, T.; Shang, R.; Nakamura, E. Iron-Catalyzed C−H Activation for Heterocoupling and Copolymerization of Thiophenes with Enamines. *J. Am. Chem. Soc.* **2022**, *144* (47), 21692−21701.

(9) Boddie, T. E.; Carpenter, S. H.; Baker, T. M.; DeMuth, J. C.; Cera, G.; Brennessel, W. W.; Ackermann, L.; Neidig, M. L. Identification and Reactivity of Cyclometalated Iron(II) Intermediates in Triazole-Directed Iron-Catalyzed C−H Activation. *J. Am. Chem. Soc.* **2019**, *141* (31), 12338−12345.

(10) Maddock, L. C. H.; Mu, M.; Kennedy, A. R.; García-Melchor, M.; Hevia, E. Facilitating the Ferration of Aromatic Substrates through Intramolecular Sodium Mediation. *Angew. Chem., Int. Ed.* **2021**, *60*, 15296−15301.

(11) (a) Tolman, C. A.; Ittel, S. D.; English, A. D.; Jesson, J. P. The Chemistry of 2-Naphthyl Bis[bis(dimethylphosphino)ethane] Hydride Complexes of Fe, Ru, and Os. 1. Characterization and Reactions with $H_2$ and Lewis Base Ligands. *J. Am. Chem. Soc.* **1978**, *100*, 4080−4089. (b) Tolman, C. A.; Ittel, S. D.; English, A. D.; Jesson, J. P. Chemistry of 2-naphthyl bis[bis(dimethylphosphino)ethane] hydride complexes of iron, ruthenium, and osmium. 3. Cleavage of sp2 carbon-hydrogen bonds. *J. Am. Chem. Soc.* **1979**, *101*, 1742−1751. (c) Baker, M. V.; Field, L. D. Reaction of sp2 carbon-hydrogen bonds in unactivated alkenes with bis(diphosphine) complexes of iron. *J. Am. Chem. Soc.* **1986**, *108*, 7433−7434. (d) Baker, M. V.; Field, L. D. Reaction of carbon-hydrogen bonds in alkanes with bis(diphosphine) complexes of iron. *J. Am. Chem. Soc.* **1987**, *109*, 2825−2826.

(12) (a) Dombray, T.; Werncke, C. G.; Jiang, S.; Grellier, M.; Vendier, L.; Bontemps, S.; Sortais, J.-B.; Sabo-Etienne, S.; Darcel, C. Iron-Catalyzed C−H Borylation of Arenes. *J. Am. Chem. Soc.* **2015**, *137* (12), 4062−4065. (b) Britton, L.; Docherty, J. H.; Sklyaruk, J.; Cooney, J.; Nichol, G. S.; Dominey, A. P.; Thomas, S. P. Iron-catalysed alkene and heteroarene H/D exchange by reversible protonation of iron-hydride intermediates. *Chem. Sci.* **2022**, *13*, 10291−10298.

(13) Camadanli, S.; Beck, R.; Flörke, U.; Klein, H.-F. C−H Activation of Imines by Trimethylphosphine-Supported Iron Complexes and Their Reactivities. *Organometallics* **2009**, *28* (7), 2300−2310.
(14) Kimura, N.; Kochi, T.; Kakiuchi, F. Iron-Catalyzed Regioselective Anti-Markovnikov Addition of C−H Bonds in Aromatic Ketones to Alkenes. *J. Am. Chem. Soc.* **2017**, *139* (42), 14849−14852.
(15) Messinis, A. M.; Finger, L. H.; Hu, L.; Ackermann, L. Allenes for Versatile Iron-Catalyzed C−H Activation by Weak O-Coordination: Mechanistic Insights by Kinetics, Intermediate Isolation, and Computation. *J. Am. Chem. Soc.* **2020**, *142*, 13102−13111.
(16) Kimura, N.; Katta, S.; Kitazawa, Y.; Kochi, T.; Kakiuchi, F. Iron-Catalyzed Ortho C−H Homoallylation of Aromatic Ketones with Methylenecyclopropanes. *J. Am. Chem. Soc.* **2021**, *143* (12), 4543−4549.
(17) For the $^{31}P/^{1}H$ NMR characterizations of complexes **1**, **3′**, **3″**, see ref 11a; for complexes $\mathbf{2_{Ph}}$, $\mathbf{4_{C6D5,D}}$, $\mathbf{4_{Ph,H}}$, see ref 11b. For complex $\{\mathbf{5^-;Na^+}\}$ see (a) Maddock, L. C. H.; Cadenbach, T.; Kennedy, A. R.; Borilovic, I.; Aromí, G.; Hevia, E. Accessing Sodium Ferrate Complexes Containing Neutral and Anionic N-Heterocyclic Carbene Ligands: Structural, Synthetic, and Magnetic Insights. *Inorg. Chem.* **2015**, *54* (18), 9201−9210 ($^{1}H$ NMR spectroscopy) and. (b) Eichhöfer, A.; Lan, Y.; Mereacre, V.; Bodenstein, T.; Weigend, F. Slow Magnetic Relaxation in Trigonal-Planar Mononuclear Fe(II) and Co(II) Bis(trimethylsilyl)amido Complexes—A Comparative Study. *Inorg. Chem.* **2014**, *53* (4), 1962−1974 ($^{57}$Fe-Mössbauer spectroscopy).
(18) (a) Salanouve, E.; Bouzemame, G.; Blanchard, S.; Derat, E.; Desage-El Murr, M.; Fensterbank, L. Tandem C−H Activation/Arylation Catalyzed by Low-Valent Iron Complexes with Bisiminopyridine Ligands. *Chem. - Eur. J.* **2014**, *20*, 4754−4761. (b) Yang, D.; Yi, H.; Chen, H.; Qi, X.; Lan, Y.; Pao, C.-W.; Lee, J.-F.; Zhang, H.; Chen, Y.-H.; Lei, A. Revealing the reduction process of Cu(ii) by sodium bis(trimethylsilyl)amide. *Faraday Discuss.* **2019**, *220*, 105−112.
(19) Crabtree, R. H. *The Organometallic Chemistry of the Transition Metals*; John Wiley & Sons, Inc.: Hoboken, NJ, 2005; pp 1−39.
(20) Banerjee, S.; Yang, Y.-F.; Jenkins, I. D.; Liang, Y.; Toutov, A. A.; Liu, W.-B.; Schuman, D. P.; Grubbs, R. H.; Stoltz, B. M.; Krenske, E. H.; Houk, K. N.; Zare, R. N. Ionic and Neutral Mechanisms for C−H Bond Silylation of Aromatic Heterocycles Catalyzed by Potassium tert-Butoxide. *J. Am. Chem. Soc.* **2017**, *139* (20), 6880−6887.
(21) Detection of smaller quantities of well-defined $Fe^0$ species when an excess of Na or K(hmds) is used (compare entries 8−9 (10 equiv M(hmds)) with entries 2−3 (2 equiv M(hmds))) is probably due to the strong reducing power of the latter, leading to the formation of higher quantities of ill-defined aggregates during the reduction course of **1**.
(22) **3***: $\delta(^{31}P)$ = 61 ppm, *d*, $J(^{31}P\text{-}^{31}P)$ = 12 Hz, to be compared with $\delta(^{31}P)$ = 60.4 ppm and $J(^{31}P\text{-}^{31}P)$ = 10 Hz for **3′**; 9.1 ppm, *m*, (7.2 ppm for **3′**). The nuclearity of **3*** has further been probed by using $^{57}$Fe-labeled starting material (Figure 1b), and a diagnostic splitting of the $^{31}P$ NMR signal of $\mathbf{^{57}Fe\text{-}3^*}$ is observed ($J(^{31}P\text{-}^{57}Fe)$ = 49 Hz, to be compared with $J(^{31}P\text{-}^{57}Fe)$ = 39 Hz for $\mathbf{^{57}Fe\text{-}4_{C6D5,D}}$), confirming that **3*** is a monometallic $Fe^0$ well-defined complex, structurally close to **3′**.
(23) (a) Gütlich, P.; Bill, E.; Trautwein, A. X. *Mössbauer Spectroscopy and Transition Metal Chemistry: Fundamentals and Applications*, 2011th ed.; Springer, 2010. (b) The isomer shift observed for this species, slightly lower than that of $\mathbf{2_{Ph}}'$ (0.19 mm/s *vs* 0.24 mm/s, Figure 1c and 2d), is also consistent with the substitution of one bromine ligand in $\mathbf{2_{Ph}}'$ by a more electron-donating hydride ligand in $\mathbf{4_{C6D5,D}}$;. (c) Herber, R. H.; Hayter, R. G. Mössbauer Effect in cis-trans Isomers. *J. Am. Chem. Soc.* **1964**, *86* (2), 301−302.
(24) Use of 12-C-4 crown-ether, which displays a better affinity for $Li^I$ cations than 15-C-5, was first used, but significant amounts of 12-C-4 ring-opening were observed. 15-C-5 however also leads to well-defined lithium adducts, in which the $Li^I$ cation is coordinated by the five O atoms from the crown ether; see Boulatov, R.; Du, B.; Meyers, E. A.; Shore, S. G. Two Novel Lithium-15-Crown-5 Complexes: An Extended LiCl Chain Stabilized by Crown Ether and a Dimeric Complex Stabilized by Hydrogen Bonding with Water. *Inorg. Chem.* **1999**, *38*, 4554−4558.
(25) Since ferration of $C_6D_6$ is still observed when the Lewis acidity of $Li^I$ is quenched by 15-C-5 crown ether, it is not excluded that formation of the C-Fe bond proceeds within a concerted metalation mechanism in which acidity of C-D bond is triggered by complexation to the iron, as $Li^I$ cations can usually enhance the acidity of such bonds by formation of $\pi$-arene complexes, see reference 20.
(26) $\mathbf{2_{Ph}}'$ was chosen as a synthetic target as no satisfying elemental analyses for the chlorinated analogue $\mathbf{2_{Ph}}$ were obtained (see SI for analytic data related to $\mathbf{2_{Ph}}'$).
(27) Liu, L.; Aguilera, M. C.; Lee, W.; Youshaw, C. R.; Neidig, M. L.; Gutierrez, O. General method for iron-catalyzed multicomponent radical cascades−cross-couplings. *Science* **2021**, *374*, 432−439.
(28) (a) Bowen, R. J.; Fernandes, M. A.; Hitchcock, P. B.; Lappert, M. F.; Layh, M. Synthesis and crystal structures of novel 1-aza-2-silacyclobut-3-enes. *J. Chem. Soc., Dalton Trans.* **2002**, 3253−3259. (b) Carravetta, M.; Concistre, M.; Levason, W.; Reid, G.; Zhang, W. Unique Group 1 cations stabilised by homoleptic neutral phosphine coordination. *Chem. Commun.* **2015**, *51*, 9555−9558.
(29) For a recent frontier article written by us on the role of such main-group cations in Fe-mediated cross-couplings, see Wowk, V.; Lefèvre, G. The crucial and multifaceted roles of main-group cations and their salts in iron-mediated cross-couplings. *Dalton Trans.* **2022**, *51*, 10674−10680.
(30) Messinis, A. M.; Luckham, S. L. J.; Wells, P. P.; Gianolio, D.; Gibson, E. K.; O'Brien, H. M.; Sparkes, H. A.; Davis, S. A.; Callison, J.; Elorriaga, D.; Hernandez-Fajardo, O.; Bedford, R. B. The highly surprising behaviour of diphosphine ligands in iron-catalysed Negishi cross-coupling. *Nat. Catal.* **2019**, *2*, 123−133.
(31) Kyne, S. H.; Lefèvre, G.; Ollivier, C.; Petit, M.; Ramis Cladera, V.-A.; Fensterbank, L. Iron and cobalt catalysis: new perspectives in synthetic radical chemistry. *Chem. Soc. Rev.* **2020**, *49*, 8501−8542.
(32) (a) Benn, R.; Lehmkuhl, H.; Mehler, K.; Rufinska, A. $^{25}$Mg-NMR: A Method for the Characterization of Organomagnesium Compounds, their Complexes, and Schlenk Equilibria. *Angew. Chem., Int. Ed.* **1984**, *23*, 534−535. (b) Gindelberger, D. E.; Arnold, J. Preparation and Properties of Magnesium, Calcium, Strontium, and Barium Selenolates and Tellurolates. *Inorg. Chem.* **1994**, *33*, 6293−6299.
(33) Uchiyama, M.; Matsumoto, Y.; Nakamura, S.; Ohwada, T.; Kobayashi, N.; Yamashita, N.; Matsumiya, A.; Sakamoto, T. Development of a Catalytic Electron Transfer System Mediated by Transition Metal Ate Complexes: Applicability and Tunability of Electron-Releasing Potential for Organic Transformations. *J. Am. Chem. Soc.* **2004**, *126* (28), 8755−8759.
(34) (a) Shen, K.; Fu, Y.; Li, J.-N.; Liu, L.; Guo, Q.-X. What are the pKa values of C−H bonds in aromatic heterocyclic compounds in DMSO? *Tetrahedron* **2007**, *63*, 1568−1576. (b) Kim, D.; Lee, G. S.; Kim, D.; Hong, S. H. Direct C(sp2)−H alkylation of unactivated arenes enabled by photoinduced Pd catalysis. *Nat. Commun.* **2020**, *11*, No. 5266, DOI: 10.1038/s41467-020-19038-8. (c) Bauer, W.; von Ragué Schleyer, P. Mechanistic Evidence for Ortho-Directed Lithiations from One- and Two-Dimensional NMR Spectroscopy and MNDO Calculations. *J. Am. Chem. Soc.* **1989**, *111*, 7191−7198.
(35) Docherty, J. H.; Peng, J.; Dominey, A. P.; Thomas, S. P. Activation and discovery of earth-abundant metal catalysts using sodium tert-butoxide. *Nat. Chem.* **2017**, *9*, 595−600.
(36) Kopf, S.; Bourriquen, F.; Li, W.; Neumann, H.; Junge, K.; Beller, M. Recent Developments for the Deuterium and Tritium Labeling of Organic Molecules. *Chem. Rev.* **2022**, *122*, 6634−6718.
(37) Gentner, T. X.; Mulvey, R. E. Alkali-Metal Mediation: Diversity of Applications in Main-Group Organometallic Chemistry. *Angew. Chem., Int. Ed.* **2021**, *60*, 9247−9262.


https://doi.org/10.1021/jacsau.3c00649
*JACS Au* 2024, 4, 512−524